

AFRL-ML-WP-TR-2007-4117

**DWELL-TIME FATIGUE CRACK
GROWTH IN Ni-BASE SUPERALLOYS**

By:

Ashok Saxena and Kip Findley

**Ashok Saxena
3539 Princeton Corners Lane
Marietta, GA 30062**

For:

**University of Dayton Research Institute
300 College Park Avenue, KL-542
Dayton, OH 45469-0104**



APRIL 2003

Final Report for 15 July 2002 – 30 April 2003

Approved for public release; distribution unlimited.

STINFO COPY

**MATERIALS AND MANUFACTURING DIRECTORATE
AIR FORCE RESEARCH LABORATORY
AIR FORCE MATERIEL COMMAND
WRIGHT-PATTERSON AIR FORCE BASE, OH 45433-7750**

NOTICE AND SIGNATURE PAGE

Using Government drawings, specifications, or other data included in this document for any purpose other than Government procurement does not in any way obligate the U.S. Government. The fact that the Government formulated or supplied the drawings, specifications, or other data does not license the holder or any other person or corporation; or convey any rights or permission to manufacture, use, or sell any patented invention that may relate to them.

This report was cleared for public release by the Air Force Research Laboratory Wright Site (AFRL/WS) Public Affairs Office and is available to the general public, including foreign nationals. Copies may be obtained from the Defense Technical Information Center (DTIC) (<http://www.dtic.mil>).

AFRL-ML-WP-TR-2007-4117 HAS BEEN REVIEWED AND IS APPROVED FOR PUBLICATION IN ACCORDANCE WITH ASSIGNED DISTRIBUTION STATEMENT.

*//Signature//

STEPHAN M. RUSS, Program Manager
Materials Behavior/Life Prediction Section
Metals, Ceramics & NDE Division

//Signature//

ROLAND E. DUTTON, Chief
Metals Branch
Metals, Ceramics & NDE Division

This report is published in the interest of scientific and technical information exchange, and its publication does not constitute the Government's approval or disapproval of its ideas or findings.

*Disseminated copies will show “//signature//” stamped or typed above the signature blocks.

REPORT DOCUMENTATION PAGE				Form Approved OMB No. 0704-0188	
<p>The public reporting burden for this collection of information is estimated to average 1 hour per response, including the time for reviewing instructions, searching existing data sources, gathering and maintaining the data needed, and completing and reviewing the collection of information. Send comments regarding this burden estimate or any other aspect of this collection of information, including suggestions for reducing this burden, to Department of Defense, Washington Headquarters Services, Directorate for Information Operations and Reports (0704-0188), 1215 Jefferson Davis Highway, Suite 1204, Arlington, VA 22202-4302. Respondents should be aware that notwithstanding any other provision of law, no person shall be subject to any penalty for failing to comply with a collection of information if it does not display a currently valid OMB control number. PLEASE DO NOT RETURN YOUR FORM TO THE ABOVE ADDRESS.</p>					
1. REPORT DATE (DD-MM-YY) April 2003		2. REPORT TYPE Final		3. DATES COVERED (From - To) 07/15/2002 – 04/30/2003	
4. TITLE AND SUBTITLE DWELL-TIME FATIGUE CRACK GROWTH IN Ni-BASE SUPERALLOYS				5a. CONTRACT NUMBER F33615-98-C-5214	
				5b. GRANT NUMBER	
				5c. PROGRAM ELEMENT NUMBER 62102F	
6. AUTHOR(S) Ashok Saxena and Kip Findley				5d. PROJECT NUMBER 4347	
				5e. TASK NUMBER 52	
				5f. WORK UNIT NUMBER 01	
7. PERFORMING ORGANIZATION NAME(S) AND ADDRESS(ES) By: Ashok Saxena 3539 Princeton Corners Lane Marietta, GA 30062				For: University of Dayton Research Institute 300 College Park Avenue, KL-542 Dayton, OH 45469-0104	
9. SPONSORING/MONITORING AGENCY NAME(S) AND ADDRESS(ES) Materials and Manufacturing Directorate Air Force Research Laboratory Air Force Materiel Command Wright-Patterson AFB, OH 45433-7750				10. SPONSORING/MONITORING AGENCY ACRONYM(S) AFRL-ML-WP	
				11. SPONSORING/MONITORING AGENCY REPORT NUMBER(S) AFRL-ML-WP-TR-2007-4117	
12. DISTRIBUTION/AVAILABILITY STATEMENT Approved for public release; distribution unlimited.					
13. SUPPLEMENTARY NOTES PAO Case Number: AFRL/WS 07-0975, 19 Apr 2007. This document contains color.					
14. ABSTRACT (Maximum 200 words) The state-of-the-art dwell-time fatigue crack growth models applicable to materials systems such as Waspaloy, Rene'95, Rene'88 and IN 100 were critically assessed. The review included models based on linear elastic fracture mechanics (LEFM) and those based on time dependent fracture mechanics (TDFM). The pertinent creep deformation and time and cycle dependent crack growth rate data on these materials were also collected to enable the evaluation of these models and for the establishment of their respective regimes of applicability and their limitations. The gaps in the available experimental and computational data for implementing the promising models were identified as part of the review. An experimental test plan and a plan for providing computational needs for addressing these shortcomings are proposed.					
15. SUBJECT TERMS fatigue crack growth, Waspaloy, Rene '95, Rene '88, IN 100, linear elastic fracture mechanics, time dependent fracture mechanics					
16. SECURITY CLASSIFICATION OF:			17. LIMITATION OF ABSTRACT: SAR	18. NUMBER OF PAGES 60	19a. NAME OF RESPONSIBLE PERSON (Monitor) Stephan M. Russ 19b. TELEPHONE NUMBER (Include Area Code) N/A
a. REPORT Unclassified	b. ABSTRACT Unclassified	c. THIS PAGE Unclassified			

Table of Contents

Section	Page
Summary and Conclusions	1
1. Introduction	3
2. Background Literature Review	5
2.1 Ni Base alloys for Aircraft Turbine Disks	5
2.2 Time-Dependent Degradation Mechanisms in Ni Base Superalloys	8
2.3 Crack Tip Parameters for Dwell-Time Fatigue Crack Growth	8
2.3.1 <i>Stress Intensity Parameter, K</i>	9
2.3.2 <i>J-Integral /ΔJ</i>	11
2.3.3 <i>Time Dependent Fracture Mechanics Parameters, C^* and C_t</i>	12
2.4 Crack Growth Models for Dwell Time Fatigue	16
2.4.1 <i>Dwell Time Crack Growth Models</i>	16
2.4.2 <i>Load Interaction Models on Crack Growth During Dwell Time</i>	18
3. Recommendations for Future Research	20
3.1 Crack Tip Parameters for Time-dependent Crack Growth in Ni base Alloys	20
3.2 Test Methods Development	23
3.3 Dwell-time Crack Growth Models	25
3.4 Models for Predicting the Effect of Load Interactions on Crack growth During Dwell Time	25
4. References	27
Appendix: Review of Fatigue, Creep, and Creep-Fatigue Data	30
• IN100	30
• Rene 95	40
• Rene 88	47
• Waspaloy	49

SUMMARY AND CONCLUSIONS

The state-of-the-art dwell-time fatigue crack growth models applicable to materials systems such as Waspaloy, Rene'95, Rene'88 and IN 100 were critically assessed. The review included models based on linear elastic fracture mechanics (LEFM) and those based on time dependent fracture mechanics (TDFM). The pertinent creep deformation and time and cycle dependent crack growth rate data on these materials were also collected to enable the evaluation of these models and for the establishment of their respective regimes of applicability and their limitations. The gaps in the available experimental and computational data for implementing the promising models were identified as part of the review. An experimental test plan and a plan for providing computational needs for addressing these shortcomings are proposed.

The microstructure of the Ni base alloys and the time dependent damage mechanisms for accumulation of creep and environmental damage have been reviewed. Both mechanisms result in intergranular crack growth thus their relative contributions are difficult to separate without conducting tests at elevated temperature under controlled environment such as varying oxygen partial pressures. Only few such studies have so far been reported. It is concluded that more experimental studies are needed to address these shortcomings.

The literature review also revealed that the elevated temperature crack growth behavior of gas turbine disk materials has been studied but relatively few studies have targeted the development of models for predicting the effects of dwell time on the fatigue crack growth behavior and the load-interaction behavior. Further, the data have been analyzed primarily using the cyclic stress intensity parameter, ΔK , for characterizing the time-dependent crack growth. This approach does not explicitly account for the evolution of crack tip stress fields due to time-dependent creep deformation and therefore, does not fully describe the crack tip conditions. Several examples of data have been used to demonstrate the limitation of the K-based approach. To analyze the data using the time-dependent fracture mechanics concepts will require measurements of the load-line displacements during the dwell periods that were not available.

The time-dependent fracture mechanics approach has primarily been developed for creep-ductile materials that possess creep strains to failure in excess of 10%. These materials behave differently from the creep-brittle materials such as Ni base alloys that have ductilities in the range of 1 to 5%. Further, Ni base alloys are also more susceptible to environmental cracking. To address these shortcomings, a systematic research program targeting the development of models for predicting the effects of dwell-time that are based on the frame-work of time-dependent fracture mechanics modified for creep-brittle materials is needed. Some preliminary work on the development of such a frame-work has been conducted on creep-brittle Al and Ti alloys that can guide the future studies. The key elements of such a research program are as follows.

- *Modifications to time-dependent fracture mechanics crack tip parameters are needed for predicting crack growth in creep-brittle materials such as*

Ni base alloys that are also sensitive to environment. This will require a combined experimental/analytical approach in which the tests conducted in laboratory will be simulated in a finite element code capable of accounting for creep and plasticity behavior as well as the effects of the growing crack on the spread of creep deformation at the crack tip. This will also yield methods for estimating the crack tip parameters in components with cracks.

- *Developments in experimental methods are needed to enable accurate measurements of load-line displacements in common test specimens such as the compact type specimen at elevated temperatures during dwell periods. The anticipated resolution of the device must be on the order of 10^{-5} mm. There are also opportunities to develop standard test methods for characterizing dwell-time crack growth behavior.*
- *Physically based models are needed to interpolate and extrapolate dwell-time effects on crack growth in applications. Such models must be based on the correct mechanisms of time-dependent crack growth in Ni base alloys and must be able to predict the effects of microstructure on the crack growth behavior.*
- *The interactions between overload and crack growth during subsequent dwell period are poorly understood and so are interactions between cyclic loads at different frequencies. A better understanding of these interactions is needed and models for predicting these effects must be developed.*

Accomplishing the above objectives will require a major interdisciplinary research effort between materials scientists, theoretical mechanics and experimental mechanics communities. Besides leading to more accurate models for crack propagation in gas turbine disks, such a program will also lay the technological basis for an ASTM standard on dwell-time fatigue crack growth behavior. Fundamental developments in fracture mechanics will result from the program that will assist in developing better approaches for prognostics for reliability of other elevated temperature systems. The program will also significantly enhance the understanding of microstructural interactions in determining crack growth behavior that will be useful in future alloy design.

1. INTRODUCTION

Turbine disks of aircraft engines are subjected to temperatures in the range of 650 °C (1200 °F) to 700 °C (1290 °F) for sustained periods during normal operation. Thus, the typical duty cycle for the disks is modeled as a fatigue stress cycle with dwell or hold time for the purposes of predicting crack initiation and propagation life as shown in Fig. 1.1 [Romanoski and Pelloux, 1990]. These service temperature is in the range where time dependent deformation due to creep and damage due to both creep and environment during the dwell period are a design and operational concern for Ni-base alloys used in this application. The period of stress relaxation at the end of take-off and during cruise in Fig. 1.1 occurs due to creep deformation. Thus, new and more accurate models are needed to predict the dwell-time effects on the fatigue crack growth behavior in turbine disk materials at elevated temperatures.

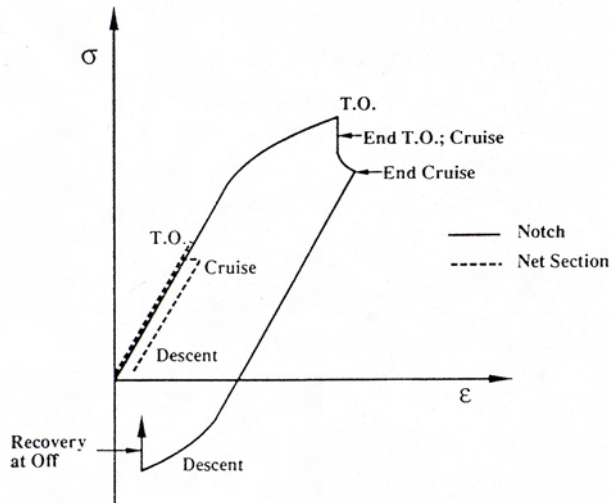


Figure 1.1- Schematic of the typical stress-strain relationship in a blade attachment section of an aircraft turbine disk during a complete take-off to landing cycle, [Romanoski and Pelloux, 1990].

Over the past two decades, several experimental studies have been conducted to characterize the elevated temperature crack growth behavior in Ni base superalloys focusing on the effects of loading frequency, temperature, microstructure, dwell time, and the effects of environment. Limited studies have also been conducted to investigate the load interaction effects when load levels and frequencies are suddenly changed or dwell periods are preceded by overloads. Consequently, substantial amounts of data are already available to guide model development. However, almost all the data have been generated within the frame-work of linear-elastic fracture mechanics (LEFM) that is unable to explicitly account for the effects of creep deformation that may play a significant role in determining the crack growth behavior and its interaction with microstructure.

Independently over the past two decades, significant analytical advances have occurred in nonlinear fracture mechanics concepts to account for creep deformation at the crack tip. A new field referred to as time-dependent fracture mechanics (TDFM) has

evolved that allows the incorporation of creep deformation effects ranging from small-scale creep to extensive creep in characterizing the crack growth behavior at elevated temperature [Saxena, 1998]. These concepts have been developed and primarily applied to elevated temperature behavior of ferritic and austenitic stainless steels that are fundamentally different from Ni base alloys. The ductility of these steels under creep conditions (10% or higher) is substantially higher than in the case of Ni base alloys (1 to 5%). Consequently, crack growth under elevated temperature conditions in these materials is always accompanied by significant creep deformation. This is not the case for Ni base alloys that are much more creep resistant and their ductility is further reduced by the presence of aggressive environment at high temperatures. Thus, crack growth in these materials is accompanied by creep strains but the magnitude of these strains is not sufficient to completely dominate over the elastic strains. Further, the presence of creep strains may be limited to the immediate vicinity of the crack tip making the stress intensity parameter, K , a valid far-field parameter. This explains some success in using K to characterize crack growth. Never-the-less, for a complete description of the crack tip conditions, the evolution of creep deformation at the crack tip must be properly represented in the crack tip parameter.

There is now an opportunity to exploit the developments in time-dependent fracture mechanics (TDFM) to develop more accurate models for predicting dwell-time effects on elevated temperature crack growth in Ni base alloys and substantially increase the confidence levels in predictions from these models. The purpose of this contract was to identify where such opportunities lie. Consequently, the objectives of the project were as follows:

- Critically review state-of-the-art dwell-time fatigue crack growth models applicable to materials systems such as Waspaloy, Rene'95, Rene'88 and IN 100 that are based on linear elastic fracture mechanics (LEFM) as well as those based on time dependent fracture mechanics (TDFM).
- Gather the pertinent creep deformation and time and cycle dependent crack growth data on the above materials to enable the evaluation of these models and for the establishment of their respective regimes of applicability and their limitations.
- Identify gaps in the available experimental and computational data for implementing the promising models and approaches and assist University of Dayton Research Institute (UDRI) and the Air Force Research Laboratory (AFRL) in developing programs to address these needs.

2. BACKGROUND AND LITERATURE REVIEW

In this section, the chemistry and microstructure of Ni base superalloys is first briefly reviewed followed by the primary time dependent degradation mechanisms during service at elevated temperature. We will then describe and critically assess the applicability of various crack tip parameters for characterizing elevated temperature fatigue, creep and creep-fatigue crack growth in these alloys followed by a description of the available models for predicting dwell-time effects on crack growth. The available crack growth data for these materials and the associated bibliography is compiled in the Appendix.

2.1 Nickel Base Alloys for Aircraft Turbine Disks

High performance materials that have a higher strength and greater corrosion resistance than martensitic steels are classified as “superalloys”. Nickel base superalloys are chosen for intermediate temperature applications such as aircraft turbine disks because of their relatively high strength at those temperatures. However, high strength also makes them more susceptible to crack growth, and an understanding of crack initiation and growth in alloys used for turbine disk material is essential.

All nickel base superalloys have a cubic, austenitic matrix phase, γ , that has an fcc crystal structure. An $L1_2$ -type ordered precipitate, γ' ($\text{Ni}_3(\text{Al,Ti})$), strengthens the matrix. The lattice parameters of γ and γ' are very similar, so the matrix and the precipitates are coherent; however, coherency strain is usually not zero and it increases the amount of hardening in the alloy [Durrand-Charre, 1997]. γ' precipitates are present as spheroidal particles when the mismatch is between 0.5 and 1 percent and they become more plate-like when the mismatch is greater than 1.25 percent [Stoloff, 1990]. Figure 2.1 shows how the γ' volume fraction has increased over the years in efforts to increase the high temperature strength of the superalloys; note the large difference between Waspaloy, Rene 95 and IN100. Figure 2.2 shows how the chemical composition of superalloys has evolved with time as the amount of Cr and the amount of γ' forming elements Al, Ti, Ta have increased [Durrand-Charre, 1997]. Turbine disks have been manufactured using superalloy powders because the microstructure in castings is too coarse to reach the strength requirements for a turbine disk.

In addition to the γ' precipitates, M_{23}C_6 and M_6C carbides are found at grain boundaries in these alloys; the carbon combines with titanium, tantalum, hafnium, and niobium to form the carbides, which can also be formed upon prolonged service exposure. M_{23}C_6 forms with moderate to high chromium content and during lower temperature heat treatment and service. When molybdenum or tungsten is more than six to eight atomic percent, M_6C forms; M_6C is important in controlling the grain size during processing. Carbides and borides, which form when boron segregates to grain boundaries, act to strengthen the grain boundaries. The borides form as blocky, half moon shaped M_3B_2 precipitates [Stoloff, 1990].

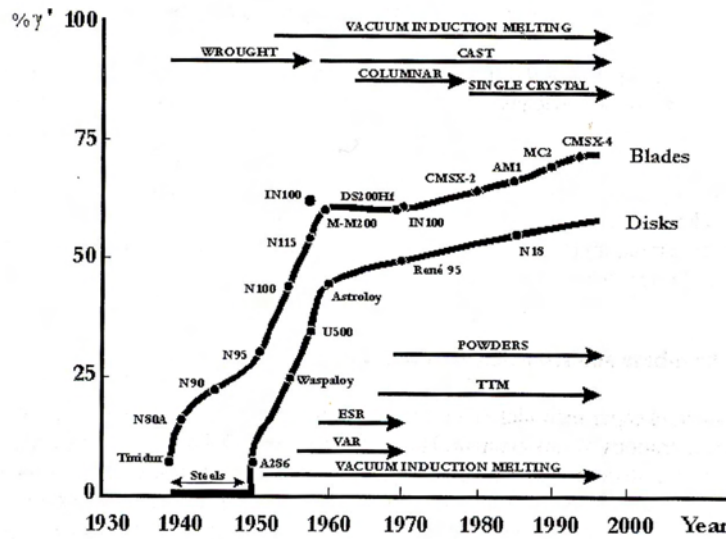


Figure 2.1- The increased volume fraction of γ' in superalloys over the years to enhance high temperature properties of blade and disk alloys [Durrand-Charre, 1997].

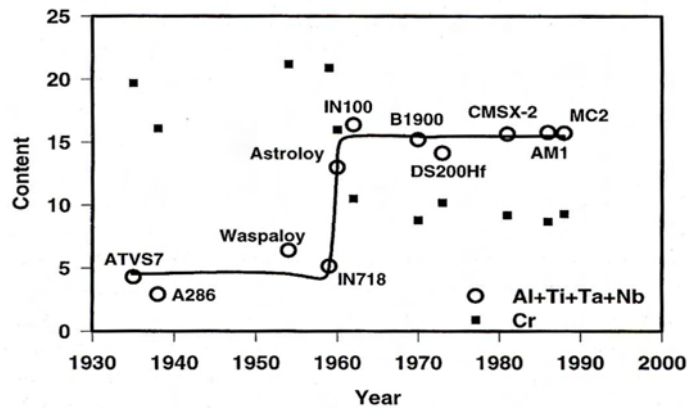


Figure 2.2- Increase in γ' forming elements and in Cr content in superalloys since the 1930s [Durrand-Charre, 1997].

Table 2.1- Nominal chemical compositions of IN100, Rene 95, and Rene 88 by weight percent [Durrand- Charre, 1997]

	C	Cr	Co	Ti	Al	Mo	B	Zr	V	W	Nb	Ni
IN100 (12)	0.18	10	15	4.5	5.5	3	0.014	0.06	1			balance
Waspaloy (13)	0.06	18.7	14.21	2.99	1.44	3.86						balance
Rene 95 (15)	0.065	13	8	2.5	3.5	3.5				3.5	3.5	balance
Rene 88 (17)	0.03	16	13	3.7	2.1	4	0.015	0.03		4	0.7	balance

Table 2.2- Role of various alloying elements in determining the properties of superalloys [Durrand-Charre, 1997]

Element	Matrix Strengthening	Increase in γ' Volume Fraction	Grain Boundaries	Other Effects
Cr	Moderate	Moderate	$M_{23}C_6$ and M_7C_3	Improves corrosion resistance; Promotes TCP phases
Mo	High	Moderate	M_6C and MC	Increases Density
W	High	Moderate		Promotes TCP phases σ and μ (Mo, W)
Ta	High	Large		
Nb	High	Large	NbC	Promotes γ' and δ phases
Ti	Moderate	Very Large	TiC	
Al	Moderate	Very Large		Improves oxidation resistance
Fe		$\gamma' \rightarrow \beta, \eta, \gamma''$ or δ		Decreases oxidation resistance; Promotes TCP phases σ , Laves
Co	Slight	Moderate in some alloys		Raises solidus; May raise or lower solvus
Re	Moderate			Retards Coarsening, Increases misfit
C	Moderate		Carbides	
B, Zr	Moderate			Inhibit carbide coarsening; Improve grain boundary strength; Improve creep strength and ductility

Table 2.1 lists the compositions of IN100, Waspaloy, Rene 95 and Rene 88. Each alloy has a different Ti/Al ratio and varying amounts of Cr. W is added to both Rene 95 and Rene 88 as a carbide former and Nb forms a fine dispersion of Nb, Ti rich precipitates in both Rene 95 and Rene 88 [Chang, 1984]. Table 2.2 shows the various effects of alloying elements on the properties of the superalloys.

There are three major constituent phases present in IN100; the first is the fcc γ matrix which is a nickel-chromium solid solution with Co and Mo substitutional atoms. The second phase, γ' , takes three forms: a fan-like phase that forms as the last liquid to solidify in the eutectic system, the primary cubic γ' (0.5-1 μm), and secondary spheres (10-100 nm). Finally, there are MC and $M_{23}C_6$ (1-5 μm) precipitates that are approximately 3-5 % of the alloy, where, M represents Ti in MC and Cr in the other precipitate [Dennison et al., 1978]. The γ' solvus is approximately 1145 $^{\circ}\text{C}$ and the volume fraction of γ' is 60 percent. Waspaloy, on the other hand, has a γ' solvus of about 1035 $^{\circ}\text{C}$; and its low Al and Ti concentrations result in a γ' volume fraction of 20 percent. These precipitates may also be smaller and more spherical [Miner et al., 1982]. Primary γ' is also present in Rene 95 as irregularly shaped particles on the grain boundaries [Bhowal, 1990]. There is no primary γ' in Rene 88 because of the supersolvus nature of its annealing treatment; as a result, there is generally a duplex distribution of γ' that is purely secondary or tertiary; the cooling γ' is secondary and the smaller, aging γ' is tertiary. If the cooling rate is sufficiently slow (less than 300 $^{\circ}\text{C}/\text{minute}$), two sizes of secondary γ' form, the second of which forms at the end of the cooling process and is similar to tertiary γ' . The secondary γ' is spherical at faster cooling rates and becomes cuboidal at cooling rates slower than 100 $^{\circ}\text{C}/\text{minute}$. Rene 88 is damage tolerant because it has the lowest γ'/γ mismatch of any commercial alloy [Wlodek et al., 1996].

2.2 Time-Dependent Degradation Mechanisms in Ni base Superalloys

The primary time-dependent degradation mechanisms in Ni base alloys at elevated temperature are creep and high temperature oxidation. The nucleation and growth of cavities at the grain boundaries due to creep result in almost purely intergranular fracture. When creep deformation is localized near the crack tip, damage in the form of grain boundary cavitation evolves ahead of the crack tip. The cavities can grow both in numbers and size and can eventually coalesce to advance the crack. Such crack growth is dominantly intergranular. The kinetics of cavity growth has been modeled as either diffusive growth or as growth constrained by the deformation of the surrounding grains. These have led to models for rationalizing the correlation between creep crack growth rates and the time-dependent fracture mechanics parameters [Wilkinson and Vitek, 1982, Bassani and Vitek, 1982, Jani and Saxena, 1987]. However, these models have no ability to predict creep crack growth rates from first principles. Never-the-less, their usefulness lies in understanding the microstructural parameters that may be pertinent to determining the creep crack growth behavior.

Environmental degradation also plays a major role in crack growth during dwell periods. Oxygen undergoes both short and long range diffusion processes in Ni base alloys at elevated temperature [A. Pineau, 1996]. An oxide layer forms at the crack tip in the short-range diffusion process, resulting in even higher stresses at the crack tip. The rupture of wedge shaped regions due to oxygen ingress from the short-range diffusion process can accelerate the intergranular crack growth rates. The long-range diffusion process involves the oxygen traveling along paths such as slip bands and grain boundaries to form internal oxide sites, cavities, or solute segregations. Figure 2.3 shows how the time-dependent crack growth rate in a Ni base alloy N18 increases significantly with oxygen partial pressure [Pineau, 1996]. In Figure 2.3a, the crack growth rate is found to be a function of the applied K level but the threshold partial pressure at which oxidation plays a significant role is independent of the applied K . Figure 2.3b shows how the temperature affects the time-dependent crack growth at various oxygen partial pressures. The temperature influences both the crack growth rate and the threshold oxygen partial pressure at which time-dependent crack growth becomes significant.

The mechanisms of creep and environment interaction are poorly understood primarily due to lack of good experimental data. Since both mechanisms produce intergranular crack growth, the only way to separate the contributions from environment and creep are to conduct crack growth tests in vacuum and by systematically varying oxygen partial pressures like in the study above. Few such studies have been reported in the literature.

2.3 Crack Tip Parameters for Dwell-Time Fatigue Crack Growth

In this section, the various fracture mechanics parameters are briefly described and a critical assessment of their ability to predict dwell-time fatigue crack growth behavior is assessed. We begin with the linear elastic fracture parameter, K and ΔK and then consider the nonlinear fracture mechanics parameters.

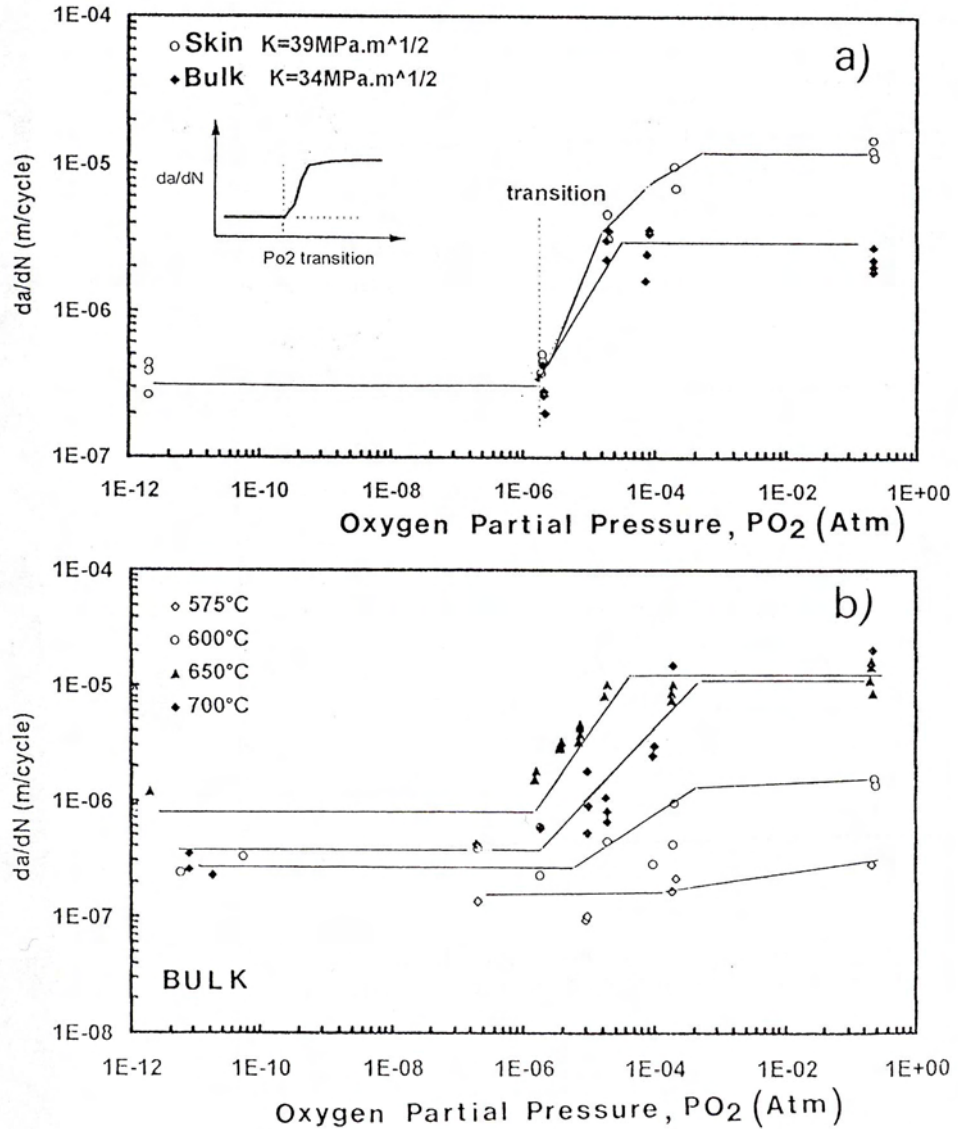


Figure 2.3. The effect of oxidation at the crack tip in alloy N18 as a function of a) the applied K value and b) temperature [Pineau, 1996].

2.3.1 Stress Intensity parameter, $K/\Delta K$

When a cracked body at elevated temperature is continuously cycled at a rapid loading frequency, such as 1 Hz or higher, and the fatigue crack growth rate is fast enough that it outpaces the spread of deformation and damage due to creep. If small-scale yielding conditions can be simultaneously maintained, the cyclic crack growth rate, da/dN , for a constant value of the load ratio, R , is uniquely correlated by the cyclic stress intensity parameter, ΔK . Experimental evidence of this correlation is provided typically

by data such as shown in Fig. 2.4 in which data from several specimens at different loads in a Cr-Mo-V steels seem to lie on a single trend [Grover, 1996].

Figure 2.5 shows the fatigue crack growth behavior of Inconel 718 at 650 °C (1200 °F) at various loading frequencies [Floreen and Kane,1980]. It is evident from this data that when cyclic frequency is decreased such that the creep and environmental effects at the crack tip are no longer negligible but small-scale yielding conditions are maintained, the crack growth rates for constant value of R also depend on the cyclic frequency, ν , in addition to ΔK . This relationship can be functionally expressed as:

$$\frac{da}{dN} = f(\Delta K, R, \nu) \quad (2.1)$$

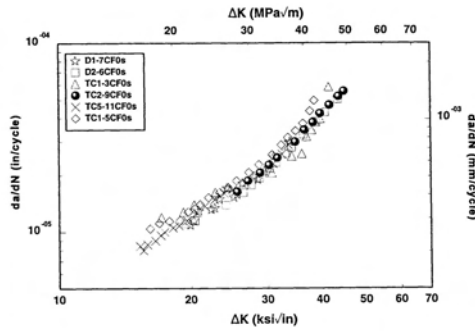


Fig. 2.4- Fatigue crack growth rate in a Cr-Mo-V steel at 594 °C (1100 °F) at a loading frequency of 1 Hz [Grover, 1996]

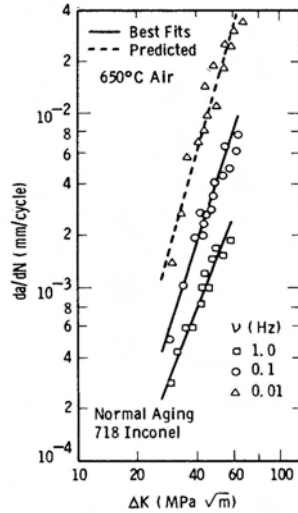


Fig. 2.5- Fatigue crack growth rate in Inconel 718 at 650 °C (1200 °F) at different loading frequencies [Floreen and Kane, 1980, and Saxena, 1984]

When a dwell (or hold) time is added to the fatigue cycle, it has been shown that in creep-ductile materials the relationship between da/dN and ΔK is no longer unique. Figure 2.6 shows an example of this behavior in a Cr-Mo-V steel showing lack of correlation [Grover, 1996, Saxena, 1998]. However, for creep-brittle materials, Figure 2.7 clearly shows that da/dN and ΔK can be correlated [Pelloux and Huang, 1980, Saxena,

1984]. Such a correlation has been rationalized using the TDFM approach that will be discuss

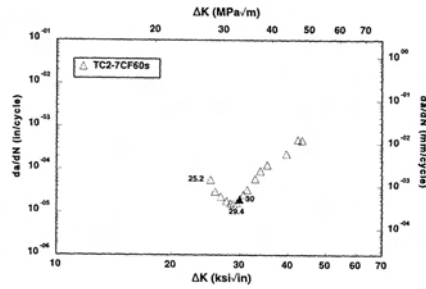


Fig. 2.6- da/dN versus ΔK behavior of a Cr-Mo-V steel at 594 °C (1100 °F) under the conditions of 60 second hold time [Grover, 1996, Saxena 1998]

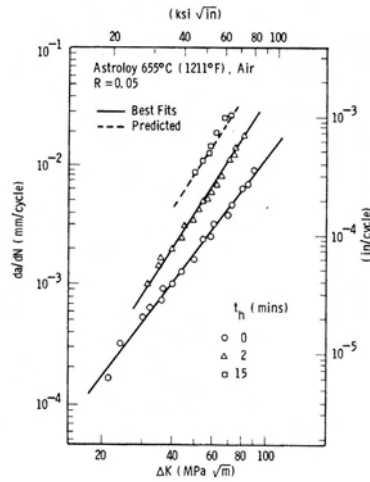


Fig. 2.7- da/dN versus ΔK behavior in Astroloy at 655 °C (1211 °F) for hold times 0, 2, and 15 minutes [Pelloux and Huang, 1980 and Saxena, 1984]

Under sustained loading conditions, large-scale creep develops at the crack tip in creep-ductile materials; therefore, creep crack growth cannot be characterized by the stress intensity parameter, K . In creep-brittle materials such as the Ni base superalloys, where the extent of the creep zone is small, K is a relevant crack tip parameter but does not uniquely characterize the crack tip conditions that are also dependent on time. Attempts have been made to correlate creep crack growth rate to K and have resulted in correlations as shown in Fig. 2.8 for IN 100 [Donath et al., 1983]. While there is some degree of correlation between creep crack growth rate and K , the hooks in the initial portion of the tests that were conducted at different loads are distinct for of each test showing that the correlations are not unique.

2.3.2 J -Integral/ ΔJ

When cyclic plasticity is no longer negligible at the crack tip, the cyclic J -integral [Dowling and Begley, 1976, Dowling, 1977], ΔJ , can be used to characterize high temperature crack growth under continuous cycling. The mathematical definition of ΔJ is given in equation 2.2 [Lamba, 1975]:

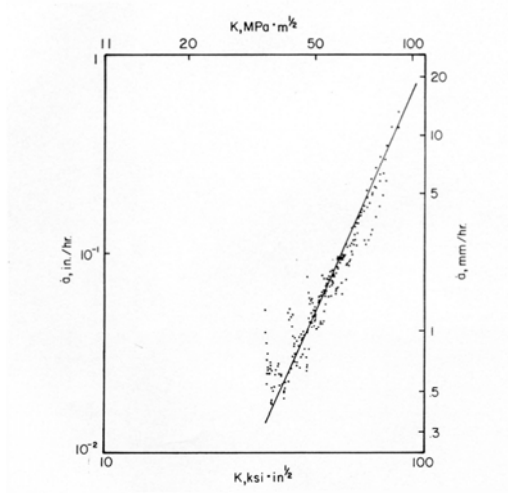


Fig. 2.8- Creep crack growth in IN-100 as function of K [Donath et al., 1983]

$$\Delta J = \int_{\Gamma} \Delta W dy - \Delta T_i \frac{\partial \Delta u_i}{\partial x} ds \quad (2.2)$$

$$\text{where, } \Delta W = \int_0^{\Delta \varepsilon_{ij}} \Delta \sigma_{ij} d(\Delta \varepsilon_{ij}) \quad (2.3)$$

$\Delta \sigma_{ij}$, $\Delta \varepsilon_{ij}$, Δu_i are the cyclic stress, strain, and displacement range, respectively, and ΔT_i = range of the applied traction vector, Γ is a counter clockwise contour that begins on the lower surface of the crack and ends on the upper surface of the crack while enclosing the crack tip. ds is a differential element along the contour Γ and x and y are the coordinates referenced to an origin at the crack tip with the x -axis aligned with the crack. All the range quantities represent the changes in those parameters as one goes from the minimum load value to the maximum load value. ΔJ is path-independent only when the stress and strain ranges are related by a univalued function. One such relationship that describes the material's cyclic stress-strain behavior is:

$$\Delta \varepsilon = \frac{\Delta \sigma}{E} + \alpha' \left(\frac{\Delta \sigma}{2\sigma_o^c} \right)^{m'} \quad (2.4)$$

In the above equation, E = elastic modulus, α' , m' are material constants obtained by regression and σ_o^c is the cyclic yield strength of the material. Since all these material constants depend on temperature, the cyclic J-integral is only a valid crack tip parameter for isothermal conditions. In the presence of temperature gradients such as during thermal fatigue, ΔJ is not expected to uniquely characterize the fatigue crack growth rates. The practical limits of the applicability of ΔJ for TMF conditions have not been fully evaluated.

2.3.3 Time Dependent Fracture Mechanics Parameters, C^* and C_I

If a cracked body is subjected to secondary creep deformation, a J-integral like path-independent integral, C^* , can be defined that uniquely characterizes the crack tip stresses and strains and can be measured at the loading pins of the body [Landes and

Begley, 1976, Saxena, 1980]. Because of steady-state conditions, the value of C^* does not vary with time for a stationary crack. If primary creep by itself dominates the behavior of the cracked body, the C^* -integral can be shown to be path-independent but its value will be a function of time and is often designated as $C^*(t)$. When small-scale or transition creep conditions prevail as is often the case in large components or in creep resistant materials such as Ni base alloys, C^* is not viable crack tip parameter because it is no longer path-independent, measurable at the loading pins, or uniquely related to the crack tip stresses and strains. C_t has been specifically proposed for those conditions and it identically reduces to C^* for the extensive creep conditions. Thus, C_t is more general and it includes all the conditions under which C^* is valid. It can be measured at the load points under small-scale creep conditions and it is shown to uniquely characterize the rate of creep zone expansion rate [Bassani et al, 1989].

Figure 2.9 shows the correlation between the time-dependent crack growth rate, da/dt , and C_t for a compact type (CT) and center crack tension (CCT) geometries [Saxena, 1986]. Figure 2.10 shows further confirmation of the validity of C_t for correlating creep crack growth rate data over a wide range of conditions ranging from small scale creep to extensive creep [Saxena, et al., 1994]. In this study, very large CT specimens were tested to promote small-scale creep conditions in the specimens for long periods allowing significant amount of data to be gathered under the small-scale creep conditions. The plot shows that regardless of whether the data were obtained under small-scale- creep or extensive creep, the trend was identical within experimental scatter.

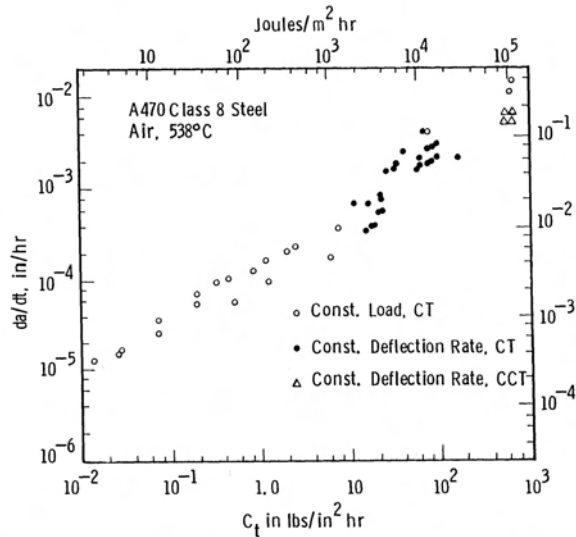


Fig. 2.9- Creep crack growth behavior in a creep-ductile, Cr-Mo-V steel at 538 °C (1000 °F) from two different specimen geometries [Saxena, 1986]

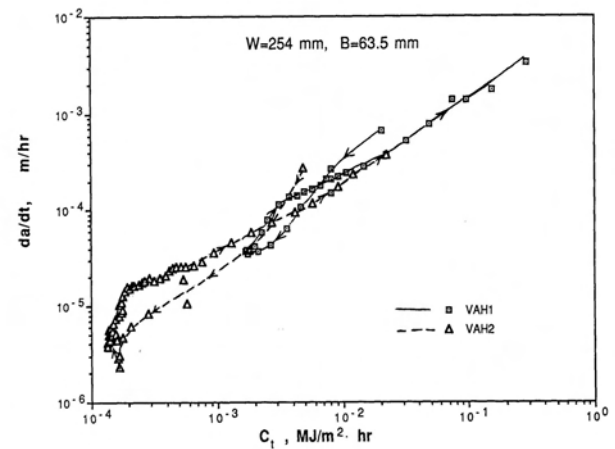


Fig. 2.10- Creep crack growth behavior in a creep-ductile, Cr-Mo-V steel under a wide range of creep conditions from small-scale to extensive creep using large specimens [Saxena,

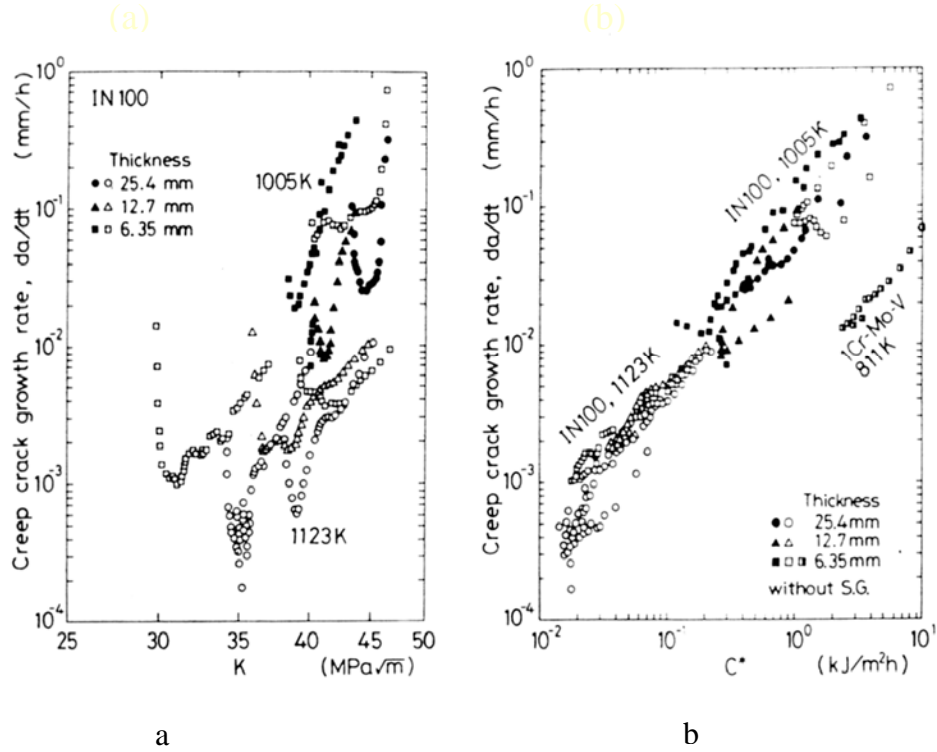


Fig. 2.11- (a) da/dt versus K data from creep crack growth tests on IN 100 conducted at different temperatures and different thickness, showing non-unique correlation with K , and b) da/dt versus C^* for the same IN100 samples showing much better correlation [Tabuchi et al., 1993]

Figure 2.11 show some recent creep crack growth data on IN 100 [Tabuchi et al., 1993] in which the data were first correlated with K , Fig. 2.11a, and finding no correlation, the data were correlated with C^* , and the correlation was much better, Fig. 2.11b. It must also be mentioned that the method by which the value of C^* is estimated for analyzing the data in Fig. 2.11b, actually estimates the value of C_t and not C^* .

We also find from Fig. 2.11 that creep crack growth data at different temperatures can be consolidated into a single trend when plotted with C^* . Similar behavior has been observed for number of other materials, e.g. in stainless steels [Saxena, 1980] and in a variety of Cr-Mo and Cr-Mo-V steels [Saxena, Han, and Banerji, 1988] and has been explained as follows. For a given applied load and specimen dimensions, the load-line displacement rate is expected to increase with temperature like the creep rate does with temperature. Thus, a C_t type parameter that depends on the product of load and the load-line displacement rate takes on a higher value at higher temperatures and thereby a higher crack growth rate is implied. Therefore, the effects of temperature on the da/dt versus C_t relationship, to the first degree, are normalized. If the basic mechanism of creep damage accumulation changes as a result of change in temperature, the da/dt versus C_t relationship is also expected to be different.

C_t for small-scale creep, $(C_t)_{ssc}$, can be measured at the loading points in test specimens and also calculated using the expressions given in equations 2.5 and 2.6. Equation 2.5 is suitable for estimating $(C_t)_{ssc}$ in specimens where both load and load-line

displacements are measured. Equation 2.6 is suitable for estimating $(C_t)_{ssc}$ in components when the load-line displacement rate must be calculated. The creep zone expansion rate, \dot{r}_c , in equation 2.6 depends on time as well as on the creep properties of the material. This equation is valid for both steady-state and primary creep or any combination of both [Saxena, 1998]. For wide range of creep conditions, C_t can be estimated by adding $(C_t)_{ssc}$ and the steady-state value of C^* as in equation 2.7.

$$(C_t)_{ssc} = \left(\frac{P\dot{V}_c}{BW} \right) F' / F \quad (2.5)$$

$$F = \frac{K}{P} BW^{1/2}; F' = \frac{dF}{d(a/W)}$$

$$(C_t)_{ssc} = \frac{2K^2(1-\nu^2)}{EW} \beta (F' / F) \dot{r}_c \quad (2.6)$$

$$\beta \approx 1/3$$

B = thickness of the specimen, W = width of the specimen, a is the crack size, P =load, E = elastic modulus, ν = Poisson's ratio, and \dot{V}_c = load-line displacement rate.

$$C_t \approx (C_t)_{ssc} + C^* \quad (2.7)$$

For materials that deform by elastic and secondary creep alone, equation 2.6 can be also written as follows [Bassani et al., 1989]:

$$(C_t)_{ssc} = \frac{4\alpha(1-\nu^2)}{E(n-1)} \beta F_{cr}(\theta, n) \frac{K^4}{W} (EA)^{\frac{2}{n-1}} \left(\frac{F'}{F} \right) t^{\frac{n-3}{n-1}} \quad (2.8)$$

$$\text{where,} \quad \alpha \approx \frac{1}{2\pi} \left(\frac{(n+1)^2}{1.38n} \right)^{\frac{2}{n-1}} \quad (2.9)$$

A , n are creep coefficient and exponent in the power-law creep behavior, $F_{cr}(\theta, n)$ is approximately 0.4 for $\theta = 90$ degrees for which the $\beta = 1/3$. The dependence of $F_{cr}(\theta, n)$ is weak on n . Thus, using equation 2.8, C_t for small-scale creep conditions can be calculated from the K-solutions and knowledge of the steady-state creep constants. This attribute of the C_t parameter is highly useful in applications.

The major limitations of C^* and C_t parameters are that they have been defined for stationary cracks only and can be applied to slow growing cracks in creep-ductile materials. Where, the term slow growing cracks applies to situations in which the creep strains accumulate at the crack tip at a rate much faster than the elastic strains associated with crack growth. In materials such as Ni base alloys that are not creep-ductile or in

those in which environment dominates the crack growth process, this assumption is no longer always satisfied. Since these materials are always in small-scale creep, has no role in characterizing creep crack growth in these materials. To apply C_t , the creep zone expansion rate in equation 2.7 must be calculated for growing cracks. This is still a topic for further research as will be discussed in Section 3 of this report.

2.4 Crack Growth Models for Dwell Time Fatigue

2.4.1 Dwell Time Crack Growth Models

Figure 2.12 schematically shows the deformation/damage zones ahead of a crack tip at elevated temperature [Saxena, 1984]. The three zones consist of the plastic zone, a creep zone and an environmentally affected zone. The plastic zone remains fixed with time for a stationery crack while the environmentally affected zone and the creep zone grow with time. The relative kinetics of the two processes must determine the one that dominates. If one assumes that environmental damage dominates the time dependent elevated temperature crack growth behavior in a material system, the following equation has been formulated to represent the dwell-time effects [Saxena, 1984]:

$$\frac{da}{dN} = c(\Delta K)^{n_1} + c_2(\Delta K)^{n_2}(\sqrt{t_h}) \quad (2.10)$$

where, n_1, n_2, C_1, C_2 are regression constants obtained from crack growth data obtained using a fast continuous fatigue cycle, and t_h is the dwell (or hold) time. This equation assumes that the time-dependent contribution to crack growth is proportional to the length of the environment affected zone which in turn is related to diffusion distance of oxygen that is proportional to the square root of time. Figure 2.7 shows the predictions of dwell-time effects using this model on Astroloy at 655 °C (1211 °F) that compare very well with the data. In this figure, the data from 0 and 2 minutes of dwell time are used to generate the constants in equation 2.10 and the rates for 15 minutes hold time are predicted and compared with the experimental data.

In creep-ductile materials, the average time rate of crack growth, $(da/dt)_{avg}$, during the dwell period is correlated with the average value of the C_t parameter, $(C_t)_{avg}$, defined in the following way.

$$\left(\frac{da}{dt}\right)_{avg} = \frac{1}{t_h} \int_0^{t_h} \left(\frac{da}{dt}\right) dt \quad (2.11)$$

$$(C_t)_{avg} = \frac{1}{t_h} \int_0^{t_h} C_t dt \quad (2.12)$$

An example of the correlation for 1.25 Cr-0.5Mo steel at 538 °C (1000 °F) is shown in Fig. 2.13 [Yoon et al., 1993]. In Fig. 2.13a, the data for various dwell times ranging from 0 to 24 hours is plotted as a function of ΔK . It is apparent that time-dependent creep deformation is more wide-spread and there is lack of correlation between crack growth rate and ΔK . The same data when plotted with $(C_t)_{avg}$ consolidates into a single trend shown in Fig. 2.13b. $(C_t)_{avg}$ can both be measured at the loading pins and be calculated by combining equations 2.5 and 2.6 with equations 2.11 and 2.12, respectively.

For the limiting case in which the creep zone during the dwell-time is completely reversed during unloading while also maintaining small-scale creep conditions, the creep fields must regenerate repetitively and become reinitialized during each cycle, $(C_t)_{avg}$, can be obtained by substituting equation 2.8 into equation 2.11:

$$(C_t)_{avg} = \frac{2\alpha(1-\nu^2)}{E} \beta F_{cr}(\theta, n) \frac{\Delta K^4}{W} (EA)^{\frac{2}{n-1}} \left(\frac{F'}{F} \right) t_h^{\frac{n-3}{n-1}} \quad (2.13)$$

From the above equation it can be seen that for a fixed hold time, the relationship between $(C_t)_{avg}$ and ΔK is unique and a correlation between da/dN and ΔK is essentially the same as one between $(da/dt)_{avg}$ which is simply equal to $1/t_h(da/dN)$ and $(C_t)_{avg}$. Thus, correlations of the type shown in Fig. 2.7 can be rationalized by time-dependent fracture mechanics concepts.

No models currently exist that will consider the synergistic effects of creep and environment damage. Neither do models exist for considering the effects of microstructure on the dwell-time effects on crack growth.

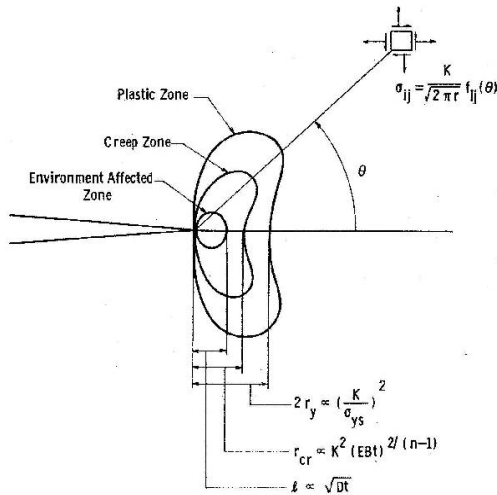


Fig.2.12- Schematic of the various zones in the region of a stationary crack showing the various deformation/damage zones ahead of the crack tip [Saxena, 1984]

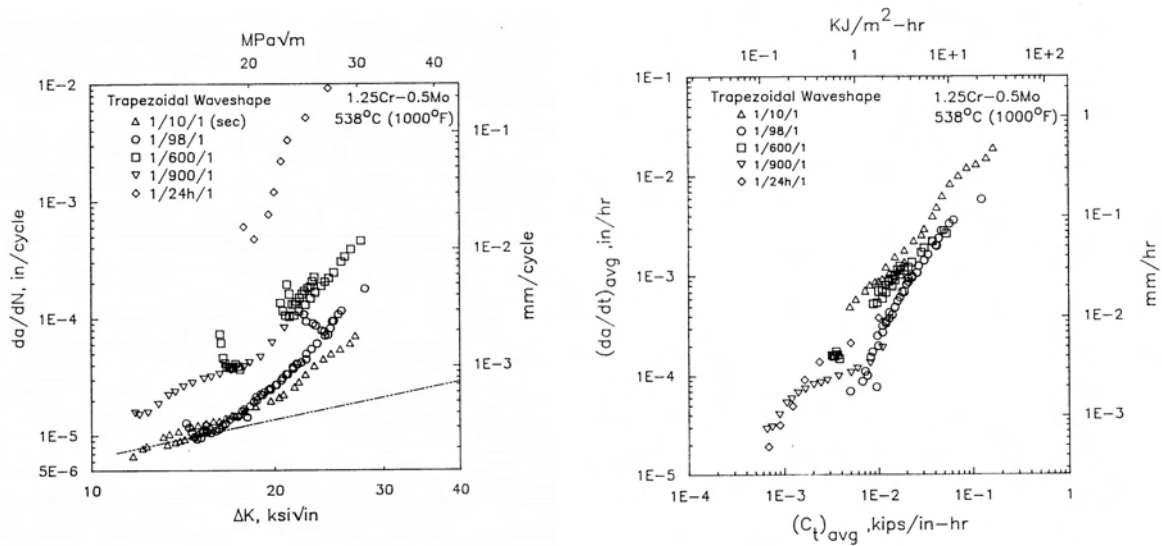


Fig. 2.13-(a) Dwell-time fatigue crack growth data expressed as function of ΔK for various hold times ranging from 0 to 24 hours for 1.25 cr-0.5 Mo steels and (b) the same data plotted in the form of $(da/dt)_{\text{avg}}$ versus $(C_t)_{\text{avg}}$ [Yoon et al., 1993]

2.4.2 Models for Predicting the Effect of Load Interactions on Crack Growth During Dwell Time

Load interaction effects have been studied on IN 100 [Larsen and Nicholas, 1983] in which hold times of 2 minutes are separated by periods of continuous cycling at various maximum K , K_{max} , values. Figure 2.14 shows the crack extension as a function of dwell time. These data clearly show that the plastic zone size developed during fatigue cycles influences the subsequent crack growth behavior during dwell time. A higher K_{max} value seems to retard the subsequent hold time crack growth rates. Crack tip plasticity reduces the stress levels at the crack tip within the plastic zone and therefore, could retard the crack growth rates during the subsequent hold time in comparison to an elastic field. The same study also presented data in which the frequency of the fatigue cycles was varied prior to application of the hold time, Figure 2.15. These data also clearly show that the dwell-time effects are influenced by the frequency of cycling.

Figure 2.16 shows the effect of prior overload on the hold time behavior of 1.25Cr-0.5Mo steels [Yoon et al., 1993a]. In these materials too, the dwell-time crack growth behavior is influenced by the prior overload. More extensive experimental studies are needed to characterize the load-interaction effects on dwell time crack growth behavior before any models can be developed. The experimental and analytical framework now exists to conduct such studies and considerably improve our understanding.

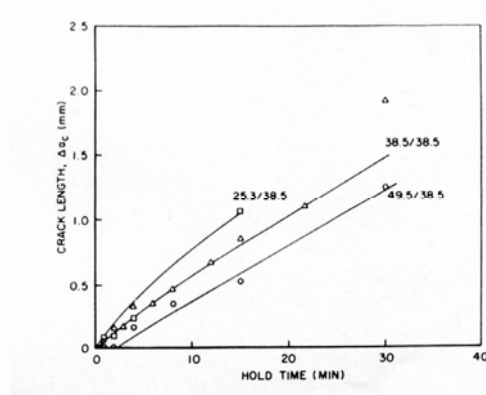


Fig. 2.14- Crack growth versus hold time for IN 100 for tests in which each hold time is preceded by continuous cycling at different values of K_{max} during cycling and the second represents the K during the hold period [Larsen and Nicholas, 1983]

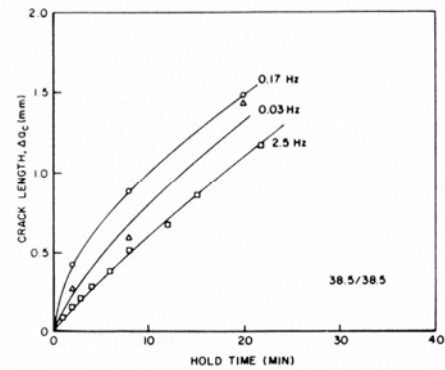


Fig. 2.15- The same as previous figure except the continuous cycling in this case was at different frequencies and K_{max} and K at hold are the same [Larsen and Nicholas, 1983]

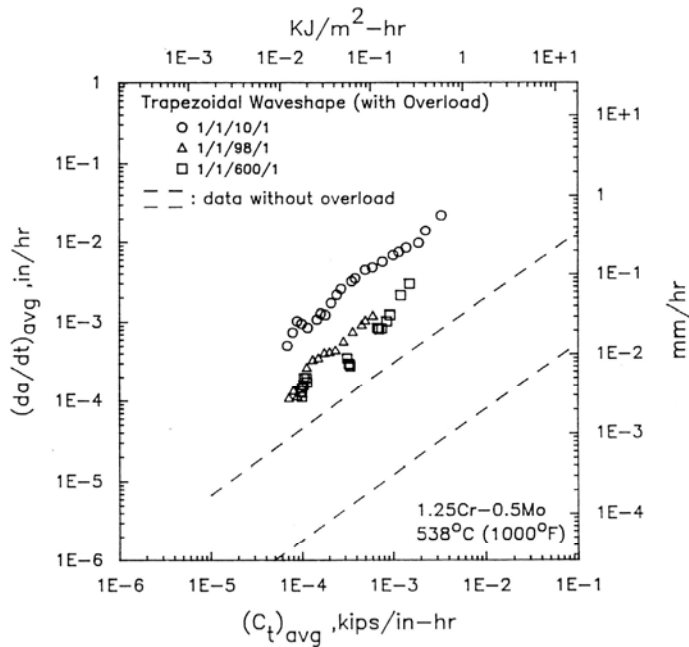


Fig. 2.16- Creep-fatigue crack growth data at various dwell-times following an overload of a factor of 2 compared to behavior with no hold time for a 1.25 cr-1 Mo steel [Yoon, Saxena, and McDowell, 1993a]

3. RECOMMENDATIONS FOR FUTURE RESEARCH

Several gaps exist in critical information/knowledge needed for developing reliable models for predicting dwell-time effects on high temperature crack growth behavior in aircraft gas turbine disks fabricated from Ni base superalloys. In this section, these shortcomings will be examined from the point of view of developing research programs that can address these issues and proposals are made for specific research to overcome them. The following distinct areas must be emphasized in future research to address the issues:

- Crack Tip Parameters for Time-dependent Crack Growth in Ni base Alloys
- Test Methods Development
- Dwell-time Crack Growth Models
- Models for Load-interaction Effects on Dwell Time Crack Growth

In the following discussion, each of these four areas is explored in depth and recommendations for specific research are made.

3.1 Crack Tip Parameters for Time-dependent Crack Growth in Ni base Alloys

As demonstrated via examples in Section 2 of the report, the stress intensity parameter, K , does not uniquely characterize the time dependent crack growth rates in Ni base superalloys. Thus, we need to examine the applicability of time-dependent fracture mechanics (TDFM) parameters. Computational methods and models for estimating nonlinear crack tip parameters are also needed to implement the models in life prediction algorithms for components.

TDFM concepts have mainly been applied to the behavior of ferritic and austenitic stainless steels at elevated temperatures as discussed in the previous section. These materials are creep-ductile in nature in which the crack growth is accompanied by large amounts of creep deformation at the crack tip. Thus, crack tip parameters such as C^* and C_t based on the assumption of stationery crack or very slow crack growth (in comparison to the kinetics of creep deformation) are successful in predicting the crack growth rate. Ni-base alloys are fundamentally different in that they exhibit much lower ductility under creep conditions. Therefore, significantly smaller amount of creep deformation in comparison to creep-ductile materials accompanies crack growth. It is therefore important to recognize that TDFM parameters may not directly be applicable to these much more complex phenomena that include creep-brittle behavior exacerbated by the effects of environment that are not a significant consideration in ferritic and austenitic steels. Combined creep and environment effects can drive the crack growth at rates that keep pace with the development of creep strains ahead of the crack tip. This condition can lead to non self-similar creep zone evolution for an extended period, thus further complicating the establishment of a single crack tip parameter for characterizing crack growth. This even brings to question whether a single parameter even exists that will

uniquely characterize the crack tip conditions and therefore the crack growth rates as demonstrated by the following example.

Sufficient understanding now exists from earlier work on aluminum alloys [Hall, 1995, Hall et al., 1998] that behave in a creep-brittle fashion to guide the future research to address the above concerns and bring closure to the questions. Figure 3.1 shows the finite element simulation of the development of crack tip creep zone in a compact type specimen of 2519 Al alloy. In this simulation, the crack tip is advanced by releasing nodes at a rate measured in an actual test conducted under loading and temperature conditions that are identical to the conditions used in the experiment. The creep zone in this case is always small in comparison the pertinent length dimensions of the specimen such as the crack size and the uncracked ligament making the applied value of K a relevant crack tip parameter. However, it is also clear that in addition to size, the shape of the crack tip creep zone is constantly evolving in this experiment questioning the uniqueness of K alone as being the crack tip parameter. Figure 3.2 shows the evolution of the creep zone along the x-axis and the y-axis clearly showing that the lack of self-similarity in the growth pattern of the creep zone. Figure 3.3a shows the correlation between creep crack growth rate and K for several specimens of 2519 Al showing that a unique correlation does not exist during the initial portion of the test during which the creep zone evolves in size and shape but the results do converge after substantial amounts of crack growth have occurred. Figure 3.3b shows the same data plotted against a K -parameter modified to include the size of the creep zone, K/r_{cA}^q , where, r_{cA} is the creep zone size for $\theta=90$ and q is a parameter that depends on the creep deformation exponent for the material. This parameter is equivalent to using C_t but defined for a growing crack [Hall et al., 1998].

In order to repeat such an analysis for Ni base superalloys, we recommend conducting 4 creep crack growth tests at the service temperature (600 °C) and simulating the test conditions in finite element analysis in ABAQUS or an equivalent code. The tests should be conducted in accordance with the latest version of the ASTM standard E-1457. The measured crack size versus time should be input as well as the creep deformation model suitable for the material and temperature. The analysis should be performed initially under plane strain or plane stress with a provision to perform a full 3-D analysis for limited conditions. The output of the analysis should provide the various crack tip parameters as a function of crack size, creep zone boundaries with crack size, and the load-line displacement as a function of time and crack size. The load-line displacement rate should be compared to the measured load-line displacement rate to ensure that the creep properties and models used in the analysis are in fact representative of the test material. To develop confidence in the crack tip parameters, it is recommended that this be repeated on a couple of other materials within the same class of turbine disk materials.

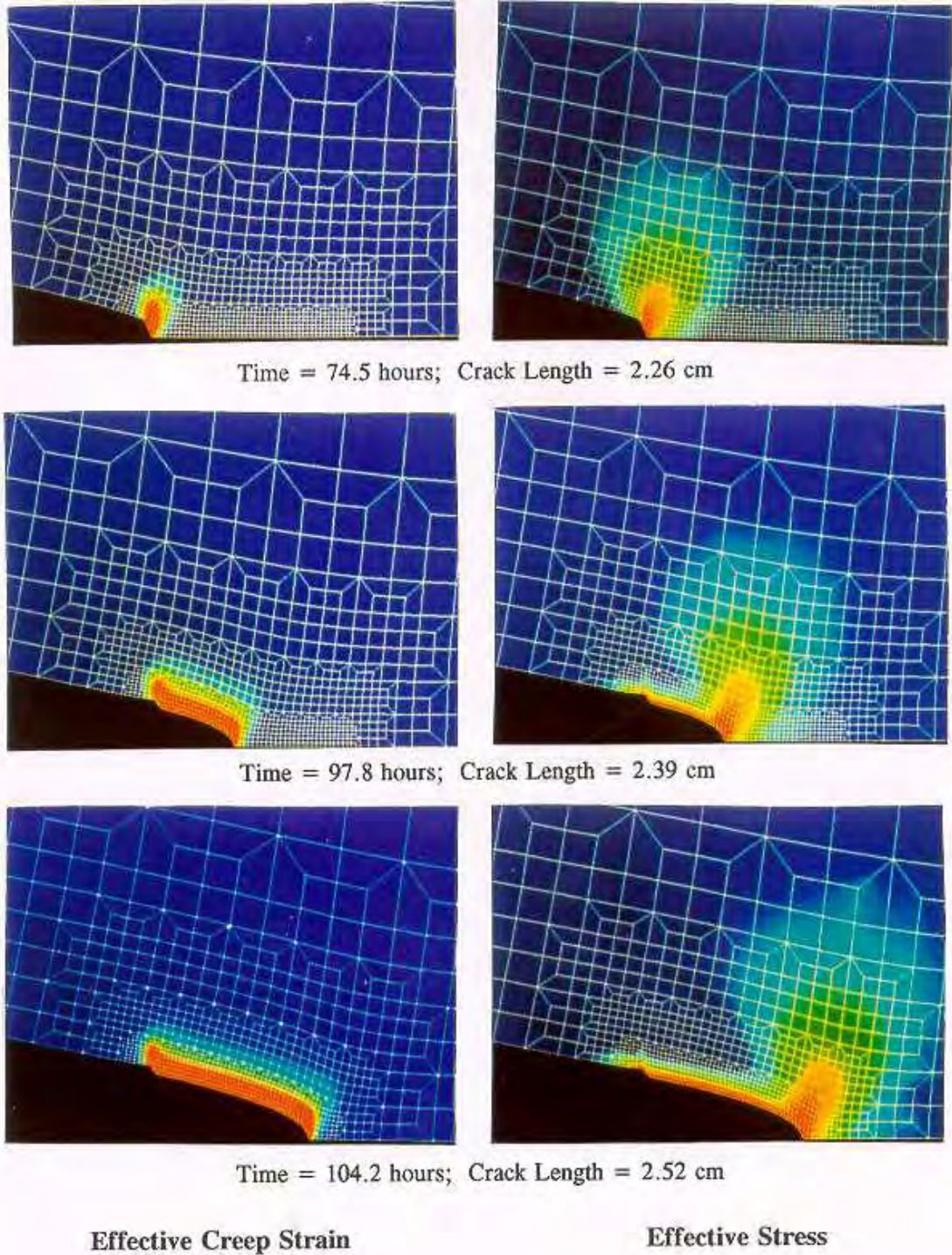


Fig. 3.1- Evolution of crack tip creep zone in a 2519 Al compact specimen at various times [Hall, 1995]. The measured crack size versus time profile was input into the analysis. Note the change in creep zone shape as a function of time [Hall, 1995].

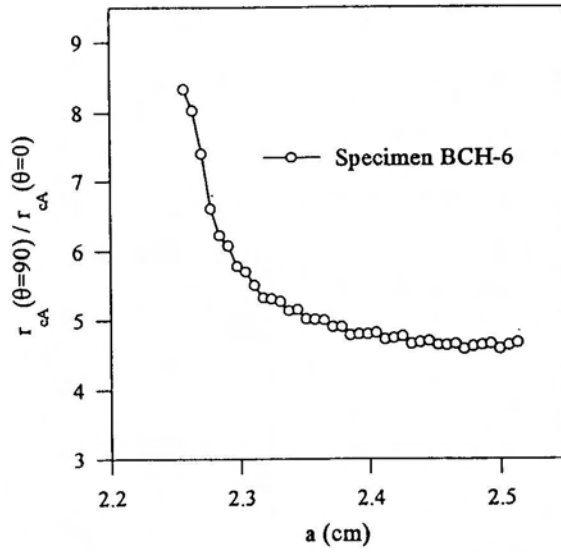
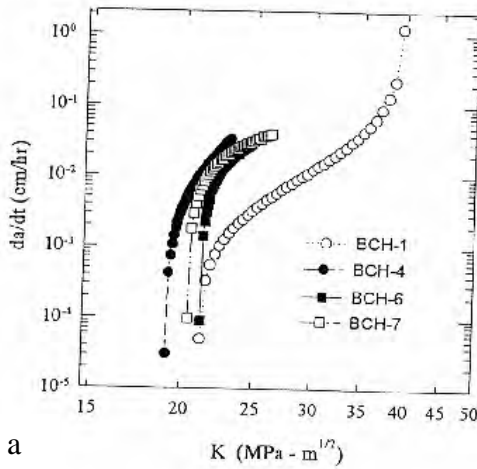
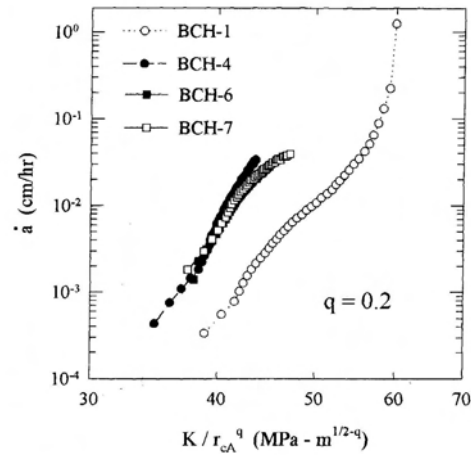


Fig. 3.2- Ratio of the creep zone size along the y-axis ($\theta = 90$) with that along the x-axis ($\theta = 0$) in the example shown in Fig. 3.1. Self-similar creep zone expansion occurs only after approximately 1.5mm crack extension [Hall et al., 1998].



a



b

Fig.3.3- (a) Creep crack growth rate as a function K for 2519 Al. The specimen BCH-1 was 6.25 mm thick while the others were 25.4mm thick (b) the same data as in (a) except correlated to K/r_{cA}^q , where r_{cA} is the instantaneous creep zone size and q is fitting constant Hall et al. 1998]

3.2 Test Methods Development

Critical developments are also needed in experimental techniques for characterizing dwell-time effects on crack growth. The highest priority need in this area

is the development of a reliable method for measuring load-line displacement at elevated temperature with a high resolution as explained below.

When LEFM frame-work is used for analyzing crack growth data, load-line displacement measurements are redundant and are, therefore, rarely made. In the TDFM frame-work, this is a key measurement that is as important as being able to measure load or crack size as a function of time. The load-line displacement contains critical information needed to estimate crack tip parameters. For example, the crack tip creep deformation behavior of the material, the information regarding the creep deformation regime such as primary, secondary or tertiary creep as well as that regarding small-scale versus extensive creep is contained in that one measurement. The lack of displacement measurement is a major limitation in being able to use existing crack growth data for implementing the TDFM approach. Considerable prior experience in extracting relevant information from load-line displacement and using it in estimating crack tip parameters and in verifying various deformation models for cracked bodies already exist. Latest contact-type and non-contact extensometers that provide repeatable and reliable resolutions in the range of 10^{-5} mm at loading frequencies of 0.1 Hz or better should be explored as explained below.

Let us use the data in Figs. 2.11 a and b to establish the desired resolution of displacement measurement needed during dwell-time testing. The C_t and $(C_t)_{avg}$ values corresponding to low end crack growth rates of interest in IN100 are in the range of 10^{-2} KJ/m²hr or 2×10^{-5} MJ/m²hr (Fig. 2.11a). This is achieved by applying load levels on compact specimens that will yield K values in the range of 30 MPa.m^{1/2} (Fig. 2.11b). The following equations are used to compute C_t and K values, respectively:

$$C_t = \frac{P \dot{V}_c}{BW} \frac{F'}{F} \quad (3.1)$$

$$K = \frac{P}{BW^{1/2}} F \quad (3.2)$$

Where, B = specimen thickness, W = specimen width, $F = K$ -calibration function and $F' = dF/d(a/W)$. Substituting the corresponding values of C_t and K into the above equations and simplifying yields,

$$\dot{V}_c = \frac{6.7 \times 10^{-7} F W^{1/2}}{F' / F} \text{ m/hr} \quad (3.3)$$

If we choose a/W value of approximately 0.4, F is approximately 8 and F'/F is approximately 4 and if choose $W = 0.0508$ m (2 in), we get \dot{V}_c as being on the order of 3×10^{-7} m/hr or 3×10^{-4} mm/hr. Thus, the accumulated deflection in 100 sec (considered to be a reasonable dwell period for laboratory testing) will be on the order of 10^{-5} mm. Thus, the deflection transducer must have at least that resolution.

Another issue with regard to test methods development is the establishment of limits for ratcheting due to plastic deformation and due to creep. Currently, there are no ASTM standards for conducting creep-fatigue crack growth testing. The critical information that is lacking for the development of such a method is the lack of a suitable displacement gage as discussed above and critical data to set limits on the allowable ratcheting of the specimen for valid creep-fatigue data. Thus, one of the objectives of the creep-fatigue tests that are proposed should be to build the necessary data on which these guidelines can be based.

3.3 Dwell-time Crack Growth Models

Creep-fatigue experiments consisting of crack growth tests using compact type specimens and single edge notch tension loaded specimens that are capable of withstanding tension and compression loading, must be conducted at hold times of 0, 10, 100, and 300 seconds. The test temperature should be the same as for creep crack growth tests, 650 °C. Some tests must also be carried out at temperatures of 600 °C and 700 °C to study the effects of environment. Tests must also be conducted under the conditions of high vacuum or inert environment to separate the effects of creep and environment on the crack growth rates. We expect that deformation data under creep, fatigue, and under creep-fatigue conditions will already be available from previous studies. However, any gaps in such data must be filled.

The mechanisms of creep and environment interaction are poorly understood primarily due to lack of good experimental data. Since both mechanisms produce intergranular crack growth, the only way to separate the contributions from environment and creep are to conduct crack growth tests in vacuum and by systematically varying oxygen partial pressures. Physics based models for creep-fatigue-environment interactions are needed that are explicitly based on realistic mechanism(s) of damage.

A key objective should be to develop models for predicting time-dependent crack growth behavior at elevated temperature and to identify the role of microstructure in developing resistance to time-dependent crack growth. Use of the state-of-the-art microstructural characterization techniques including scanning electron microscopes (SEM), transmission electron microscopes (TEM) to characterize the microstructure and to use advanced stereological techniques to quantify all relevant aspects of the microstructure. The characterization should be performed on original microstructures as well as on microstructures after exposure to elevated temperatures. A detailed characterization of the crack path and its interaction with microstructure must be performed to support the effort of identifying the crack growth mechanisms.

3.4 Models for Predicting the Effect of Load Interactions on Crack growth During Dwell Time

There are only a few studies reported in the literature on the effects of prior overload on the effects of dwell-time at elevated temperature [Yoon et al., 1993a and

Larsen and Nicholas, 1983]. Plastic deformation at the crack tip is known to influence the growth of the creep zone [Yoon et al., 1992] and therefore the magnitude of the C_I parameter. Thus, overload is expected to influence crack growth rates during dwell time. However, it also makes intuitive sense that the overload effects on crack growth rate during dwell-time decrease with increasing hold time and will be most important during the initial periods of the hold time. It is therefore suggested that creep-fatigue crack growth tests be conducted with same hold time as in previous task but following overloads ranging from 25 % to 100%. Measurement of load-line displacement rates immediately following the hold time will be critical in understanding the effects of overload. It is also recommended that finite element simulations of the actual loading be performed to assess the behavior of the creep zone expansion at the crack tip following the application of the overload.

4. REFERENCES

- J.L. Bassani, D. E. Hawk and A. Saxena, 1989 "Evaluation of the C_t Parameter for Characterizing Creep Crack Growth in the Transient Regime", in *Nonlinear Fracture Mechanics: Time-Dependent Fracture Mechanics*, Vol. I, ASTM STP 995, ASTM, Philadelphia, pp. 7-29.
- J.L. Bassani and V. Vitek, 1982, "Propagation of Cracks Under Creep Conditions", *Proceedings of the 9th National Congress of applied Mechanics- Symposium on Nonlinear Fracture Mechanics*, pp. 127-133.
- P.R. Bhowal, E.F. Wright, E.L. Raymond, 1990, "Effects of Cooling Rate and Gamma Prime Morphology on Creep and Stress-rupture Properties of a Powder Metallurgy Superalloy," *Metallurgical Transactions A - Physical Metallurgy and Materials Science*, vol. 21A, pp. 1709-1717.
- D.R. Chang, D.D. Krueger, R.A. Sprague, 1984, "Superalloy Powder Processing, Properties and Turbine Disk Applications," *Superalloys 1984; Proceedings of the Fifth International Symposium, Champion, PA*, pp. 245-273.
- J.P. Dennison, P.D. Holmes, B. Wilshire, 1978, "The Creep and Fracture Behavior of the Cast, Nickel-based Superalloy, IN100," *Materials Science and Engineering*, Vol. 33, pp. 35-47.
- R.C. Donath, T. Nicholas, and L.S. Fu, 1981, "An Experimental Investigation of Creep Crack Growth in IN100," *Fracture Mechanics: Thirteenth Conference*, ASTM STP 743, pp. 186-206.
- N.E. Dowling, 1977, "Crack Growth During Low-Cycle Fatigue of Smooth Axial fatigue Specimens", in *Cyclic stress-Strain and Plastic Deformation Aspects of fatigue Crack Growth*, ASTM STP 637, ASTM, Philadelphia, pp. 97-121.
- N.E. Dowling and J.A. Begley, 1976, "Fatigue Crack Growth Under Gross Plasticity and the J-Integral", in *Mechanics of Crack Growth*, ASTM STP 590, ASTM, Philadelphia, pp. 82-103
- M. Durand-Charre, 1997, The Microstructure of Superalloys, Gordon, Breach Science Publishers.
- S. Floreen and R.H. Kane, 1980, "An Investigation of the Creep-Fatigue-Environment Interaction in a Ni Base Alloy", *Fatigue of Engineering Materials and Structures*, Vol. 2, pp. 151-164
- P.S.Grover, 1996, "Creep-Fatigue Crack Growth in Cr-Mo-V Base Material and Weldments", Ph.D. Dissertation, Georgia Institute of Technology, Atlanta, GA.
- D.E. Hall, 1995, "Analysis of Crack growth in Creep-Brittle Materials", Ph.D. Dissertation, Georgia Institute of Technology, Atlanta
- D.E. Hall, D.L. McDowell, and A.Saxena, 1998, "Crack Tip Parameters for Creep-Brittle Crack Growth", *Fatigue and Fracture of Engineering Materials and Structures*, Vol.21, pp. 387-401.
- S.C. Jani and A.Saxena, 1987, "Influence of Thermal Aging on the Creep Crack Growth Behavior of a Cr-Mo Steel", *Effects of Thermal and Load Histories*, TMS, pp. 201-220.
- H.S. Lamba, 1975, "The J-Integral Approach to Cyclic Loading", *Engineering Fracture Mechanics*, Vol.7, pp. 693-703.
- J.D. Landes and J.A. Begley, 1976, "A Fracture Mechanics Approach to Creep Crack Growth", in *Mechanics of Crack Growth*, ASTM STP 590, ASTM, Philadelphia, pp. 128-148.

- J.M. Larsen, T. Nicholas, 1983, "Load Sequence Crack Growth Transients in a Superalloy at Elevated Temperature," *Fracture Mechanics, Fourteenth Symposium – Volume II: Testing and Applications*, ASTM STP 791, vol. II, pp. II-536-II-552.
- R.V. Miner, J. Gayda, R.D. Maier, 1982, "Fatigue and Creep-fatigue Deformation of Several Nickel-base Superalloys at 650 C," *Metallurgical Transactions A - Physical Metallurgy and Materials Science*, vol. 13A, pp. 1755-1765.
- R.M. Pelloux and J.S. Huang, 1980, "Creep-Fatigue-Environment Interactions in Astroloy", Creep-Fatigue-Environment Interactions, R.M. Pelloux and N.S. Stoloff editors, TMS-AIME, pp. 151-164.
- A. Pineau, 1996, "Fatigue and Creep-Fatigue Behavior of Ni-Base Superalloys: Microstructural and Environmental Effects," *Mechanical Behavior of Materials at High Temperature*, Kluwer Publishers, Holland, pp. 135-154.
- G.R. Romanoski Jr., R.M. Pelloux, 1990, "The Fatigue Behavior of Small Cracks in an Aircraft Turbine Disk Alloy," Elevated Temperature Crack Growth; Proceedings of the Symposium, ASME Winter Annual Meeting, Dallas, TX, pp. 7-23.
- A. Saxena, 1980, "Evaluation of C^* for Characterization of Creep Crack growth Behavior of 304 Stainless-Steel", in *Fracture Mechanics, Twelfth Conference*, ASTM STP 700, ASTM, Philadelphia, pp. 131-151.
- A. Saxena, 1984, "A Model for Predicting the Environment Enhanced fatigue Crack Growth Behavior at High Temperature", in *Thermal and Environmental Effects in Fatigue-Research Design Interface- PVP-71*, ASME, New York, pp. 171-184
- A. Saxena, 1986, "Creep Crack Growth Under NON Steady-State Conditions", in *Fracture Mechanics, Seventeenth Volume*, ASTM STP 905, ASTM, Philadelphia, pp. 185-201.
- A. Saxena, *Nonlinear Fracture Mechanics for Engineers*, CRC Press, 1998
- A. Saxena, J. Han and K. Banerji, 1988, "Creep Crack Growth behavior in Power-Plant Boiler and Steam Pipe Steels", *Journal of Pressure Vessel and Technology*, ASME, Vol. 110, pp. 137-146.
- A. Saxena, K. Yagi, and M. Tabuchi, 1994, "Crack Growth Under Small-Scale and Transition Creep Conditions in Creep-Ductile Materials" in *Fracture Mechanics: Twenty-Fourth Volume*, ASTM STP 1207, ASTM, Philadelphia, pp. 481-497.
- N.S. Stoloff, 1990, "Wrought and P/M Superalloys," *ASM International, Metals Handbook*, Vol. 1, pp. 950-977.
- M. Tabuchi, K. Kubo, K. Yagi, 1993, "Creep Crack Growth of Creep Brittle Alloy," *Creep and Fracture of Engineering Materials and Structures, Swansea, UK, 28 Mar.-2 Apr. 1993*, pp. 449-458.
- D.L. Wilkinson and V. Vitek, 1982, "Propagation of Cracks by Cavitation—a General Theory", *Acta Metallurgica*, Vol. 30, pp. 1723-1732.
- S.T. Wlodek, M. Kelly, D.A. Alden, 1996, "The Structure of Rene 88 DT," *Superalloys 1996; Proceedings of the 8th International Symposium*, Champion, PA, pp. 129-136.
- K.B. Yoon, D.L. McDowell, and A. Saxena, 1992, "Influence of Crack Tip Plasticity on Creep-Fatigue Crack Growth, in *fracture Mechanics: Twenty Second Symposium*, (Vol. I), ASTM STP 1131, ASTM, Philadelphia, pp. 367-392.
- K.B. Yoon, A. Saxena, and P.K. Liaw, 1993, "Characterization of Creep-Fatigue Crack growth Behavior Under Trapezoidal Waveform using C_t -Parameter", *International Journal of Fracture*, Vol. 59, pp. 95-114.

K.B. Yoon, A.Saxena, and D.L. McDowell, 1993a, "Effect of Cyclic Overload on the Crack Growth Behavior during Hold Period at Elevated Temperature", *International Journal of Fracture*, Vol. 59, pp. 199-211.

Appendix

Review of Available Fatigue, Creep, and Creep-Fatigue Crack Growth Data

In this Appendix, the available crack growth data on Ni base alloys used in turbine disks such as IN100, Rene 95, Rene 88 and Waspaloy and the background creep deformation and crack growth data are presented. Several of the plots from this data collection are also used in the main body of the report to discuss models for dwell-time effects on crack growth. A complete bibliography of references is also included in this Appendix for each material.

IN100

Because of its broad use in the aircraft engine industry, a large amount of high temperature data exists for IN100. Dennison et al. [Dennison et al., 1978] found that steady-state creep rate, $(d\epsilon/dt)_s$, in IN100 increases with increased temperature and they initially fit the following equation to the data:

$$(d\epsilon/dt)_s = A\sigma^n \exp(-Q_c/RT) \quad (A1)$$

where, A , n , Q_c are regression constants, R = Universal gas constant, and T = is the absolute temperature. They found that the value of n is different for different values of applied stress, and the activation energy, Q_c , is dependent on temperature (Fig. A1) so they modified the equation for representing the steady-state creep rate:

$$(d\epsilon/dt)_s = A^* (\sigma - \sigma_0)^p \exp(-Q_c^*/RT) \quad (A2)$$

σ_0 in the above equation is dependent on the temperature and microstructural features such as subgrain size, solute-dislocation interactions, and the presence of a dispersion of particles in the matrix. A^* , p , and Q_c^* are new values of A , n , and Q_c that appear to be independent of applied stress and temperature. σ_0 is approximately equal to the yield strength of the material at a similar temperature and at a strain rate equal to the steady-state creep rate. The steady-state creep rate increases with increased stress and temperature (Figure A2). In two phase materials such as IN100, σ_0 may be large and decreases with increasing temperature.

Dennison et al. also performed experiments where IN100 was annealed at the aluminizing temperature every 150 ks, but found there is only a minor improvement in creep life with the heat treatments (Figure A3). A small amount of primary creep is present after every heat treatment and there is a slightly more extensive primary stage, but the procedure results in no significant improvement in creep life

Figure A4 shows IN100 creep data [Dennison et al., 1978]. Figure A4a plots the time to rupture for two test temperatures as a function stress. Also shown are the

minimum creep rates for two different temperatures at different stress values (Figure A4b), percent elongation as a function of time to rupture at two different temperatures (Figure A4c), and reduction of area as function of time to rupture at two different temperatures (Figure A4d).

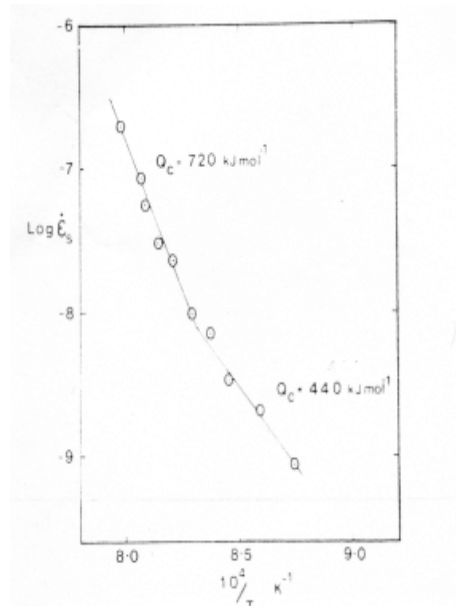


Figure A1. Steady state creep rate (s⁻¹) as a function of temperature at a stress level of 185 MPa for IN100 ($d\epsilon/dt = A\sigma^n \exp(-Q_c/RT)$) [Dennison et al., 1978].

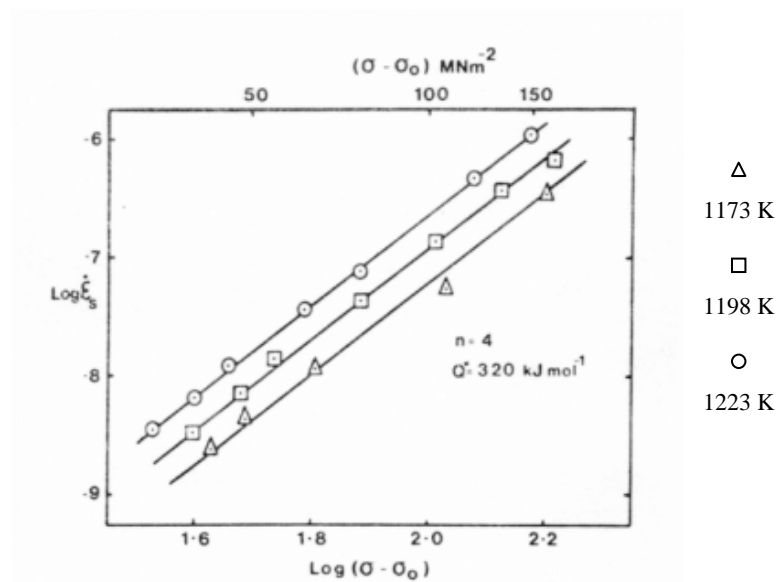


Figure A2. Temperature dependence of the relationship between the steady-state creep rate and $(\sigma - \sigma_0)$ in IN100 based on a dislocation network growth model [Dennison et al., 1978]

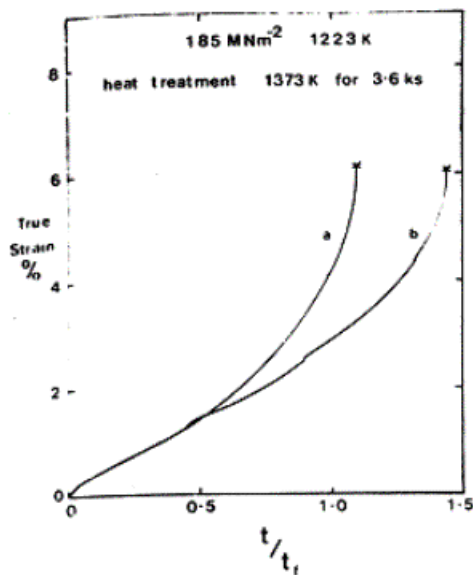


Figure A3- Creep curves for IN100 specimens tested at 185 MPa and 1223K where (a) is for an interrupted test and (b) is for a specimen that was annealed for 3.6 ks at 1373K after every 150 ks period of creep [Dennison et al., 1977].

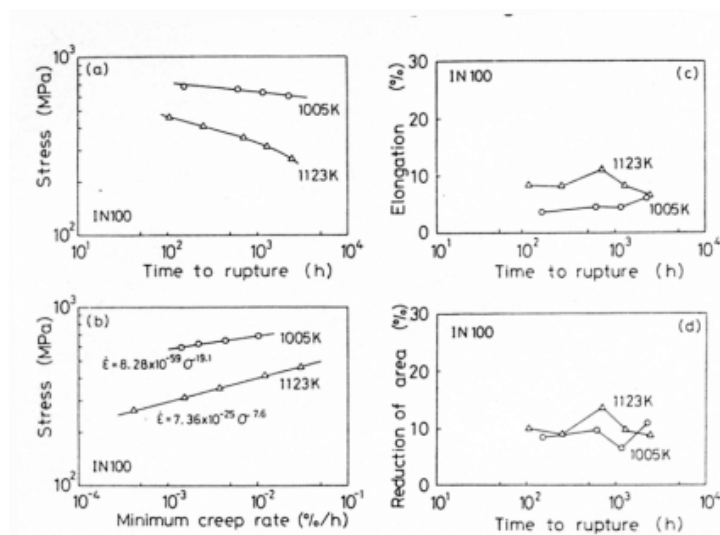


Figure A4-a) Stress versus time to rupture, b) stress versus minimum creep rate, c) elongation versus time to rupture, d) reduction of area versus time to rupture for creep tests of IN100 round bar specimens conducted at 1005K and 1123K [Tabuchi et al, 1993].

Figure A5 shows da/dt versus K for IN100 tested at 732°C [Donath, Nicholas, and Fu, 1981]. The scatter on the plot demonstrates that there are nonunique trends in the da/dt versus K behavior. Also, the magnitude of the initial crack growth rate is about double of the steady-state creep rate that result in the “hooks” on the da/dt versus K plot [Donath, Nicholas, and Fu, 1981].

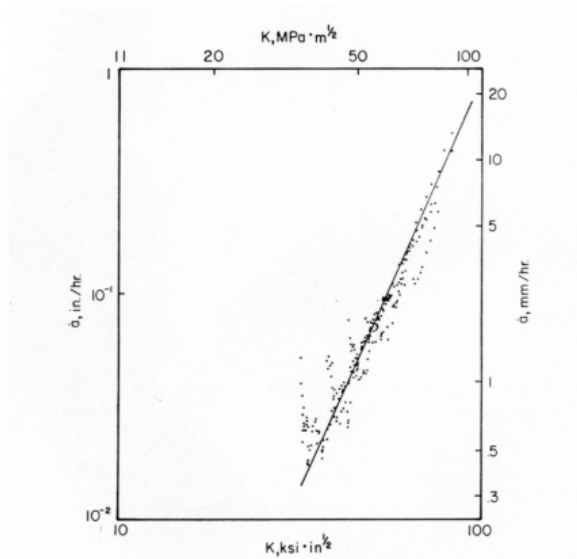


Figure A5- da/dt versus K for a 7/32 inch thick IN100 CT specimen showing non-unique trends in the correlation [Donath, Nicholas, and Fu, 1981]

As sample thickness increases, da/dt for the same value of K increases (Figure A6), which is due to the development of enhanced plasticity and creep around the crack tip of thinner specimens. However, when C^* is used as the fracture parameter, there is no significant variation of crack growth rate with thickness (Figure A7) because C^* accounts for the development of creep in the crack tip region. The enhanced creep rates in the thin specimens are reflected in the measured load-line deflection rate and therefore in the estimated value of C^* . Figure A8 compares da/dt data vs. K and C^* at different temperatures and with specimens of different thickness; when da/dt is plotted against K , there is large amount of scatter in the data, even at 1005 °C where IN100 is very brittle. When da/dt is plotted against C^* , most of the scatter disappears because C^* accounts for the crack tip creep conditions. Also of note is that the da/dt values at 1005 °C are slightly higher than the da/dt values for 850 °C (1123 K) because the γ' structures at those temperatures are not the same, which results in a difference of ductility in the material.

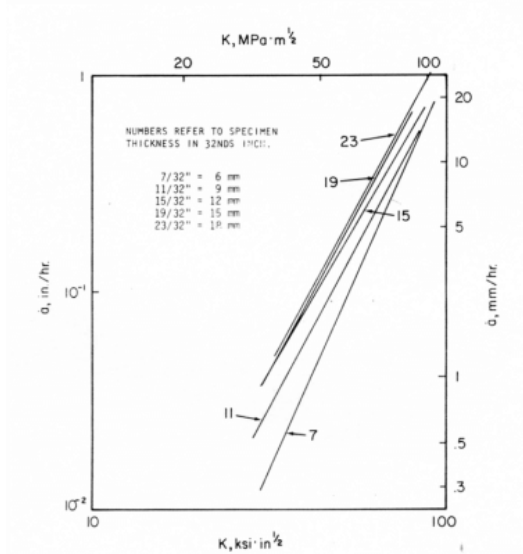


Figure A6- da/dt versus K data showing variation in crack growth rate for different IN100 sample thickness [Donath, Nicholas, and Fu, 1981] .

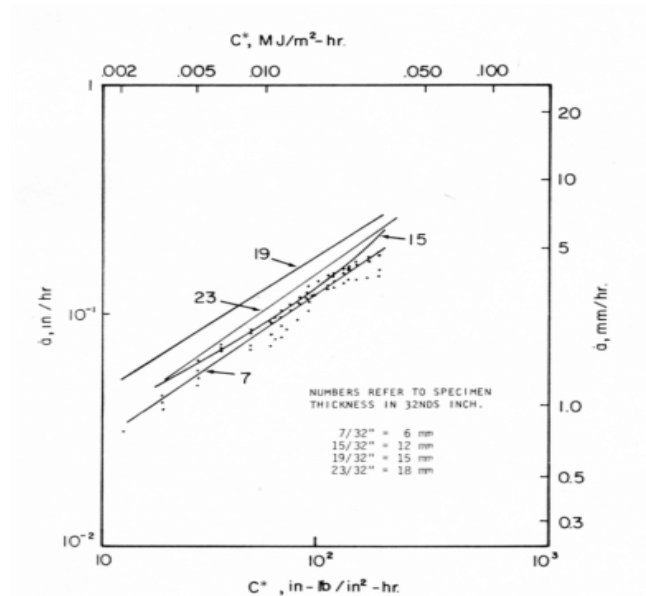


Figure A7- da/dt versus C^* data for IN100 specimens which has better correlation than the da/dt versus K data [Donath, Nicholas, and Fu, 1981].

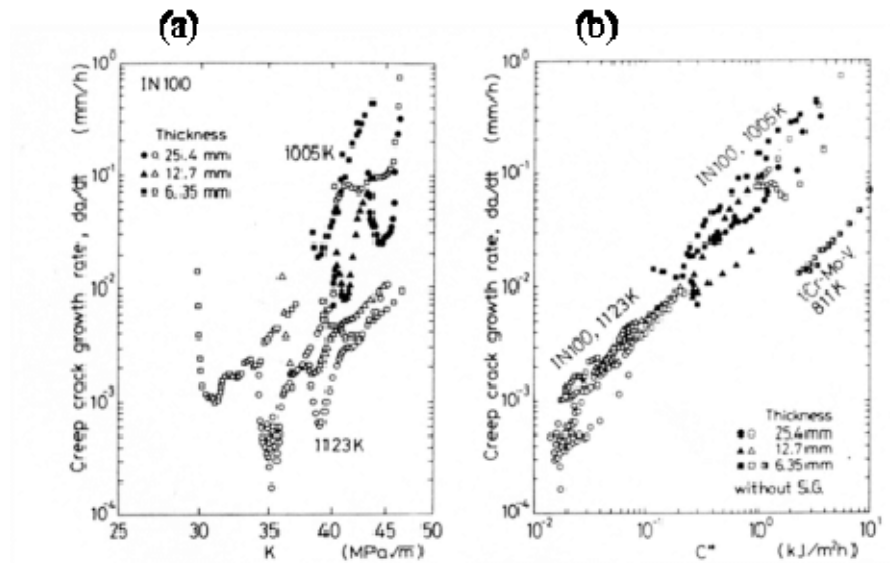


Figure A8- a) da/dt versus K data for creep crack growth tests done at different temperatures with IN100 specimens of different thickness, showing non-unique solutions and significant scatter in the trend; b) da/dt versus C^* for IN100 samples of different thickness tested at different temperatures, showing much less scattering. 1Cr-Mo-V data is also included on the plot.

Creep-fatigue-environment interactions in IN100 are important for predicting dwell-time effects; depending on the load, cycling frequency, temperature, and several other parameters, the interaction between creep, fatigue, and environment can change drastically.

Figure A9 shows da/dt versus K_{max} for specimens of various thickness tested at 732°C. The samples with shallower side grooves showed a slightly greater crack growth

rate than the specimens with deeper grooves; there is some variation in the data as thickness and the initial stress intensity loading change.

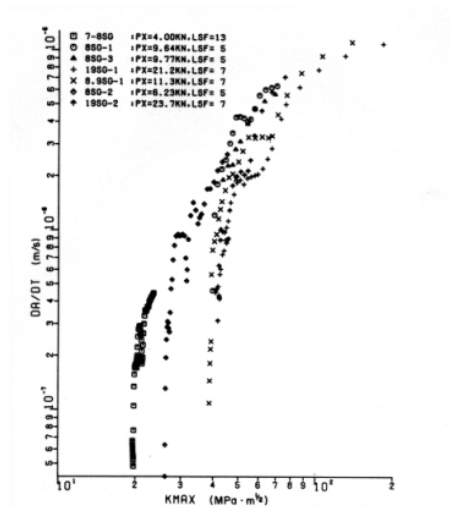


Figure A9-Crack growth rates for IN100 specimens of different thickness and initial stress intensity loadings.

In order to simulate service loadings, specimens are often fatigued at a high temperature for a set amount of time, held at a constant load, and then cycled under fatigue again; the process continues until the required data are obtained. When there are high stress intensity levels around the crack tip, the crack grows at a uniform rate at each hold time duration (Figure A10). When stress intensity at the crack tip decreases, the initial crack growth rate becomes greater than the steady-state crack growth rate as seen in Figure A10 [Larsen and Nicholas, 1983]. During fatigue with hold time, the relative values of the K_{max} for fatigue and hold time and their effect on crack initiation and growth is notable (Figure A11). When the value of K_{max} for the hold time is less than that for fatigue, there is an incubation time before crack growth begins. On the contrary, if the stress intensity factor for fatigue is less than or equal to the stress intensity factor for hold time, crack growth begins immediately at the beginning of the hold time. The frequency of fatigue before the hold time may be a major factor in determining what the dominant driving forces for crack growth are: creep, fatigue, and/or environment. Crack length versus hold time data after the application of different frequencies of fatigue show that the initial crack growth rate increases as the previously applied frequency of fatigue decreases (Figure A12); possibly, the fatigue cycling at higher frequencies overshadows the time-dependent crack growth processes while at lower frequencies, the environment increases crack growth rate, though the creep effects are negligible. Thus, the stresses around the crack tip remain high and crack tip damage is a maximum. At the lowest frequencies, the environment still enhances crack growth rate, but there is more time for creep to relax the stresses around the crack tip so the crack tip damage is less severe. After holding, the crack will not begin growing again until the specimen has undergone a certain number of cycles, which are called delay cycles. The delay cycles are due to the nonuniform creep crack growth rate and retardation of fatigue crack growth rate

following creep crack growth. The number of delay cycles increases most rapidly at shorter hold times and begins to saturate afterwards (Figure A13). Figure A14 demonstrates how the number of cycles in the segments surrounding a hold time affects the mechanism that drives the crack growth. If the number of cycles between the hold time segments is greater than 20, the average da/dt is approximately equal to the da/dt for pure fatigue. The linear cumulative damage hypothesis predicts crack extension is the linear summation of crack growth from steady-state fatigue and steady-state creep with no interaction effects; however, this hypothesis predicts crack growth rates that are smaller than the experimental data, which suggests there is an interaction between fatigue and creep crack growth [Larsen and Nicholas, 1983].

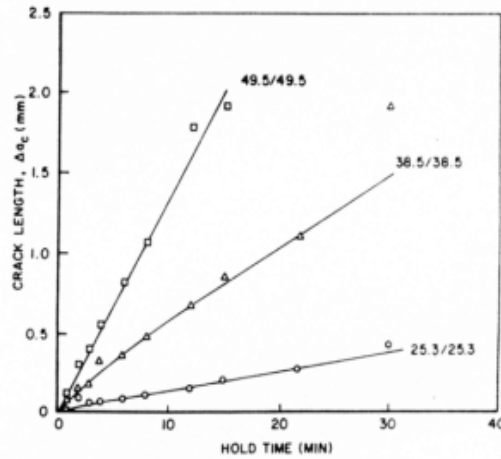


Figure A10- Crack growth during hold times measured on the fracture surface of the IN100 specimens; the first number for each data set represents the maximum stress intensity ($\text{Mpa}\cdot\text{m}^{1/2}$) for the fatigue cycling ($R = 0.1$) before and after the hold time, while the second number represents the stress intensity level applied during the hold time [Larsen and Nicholas, 1983].

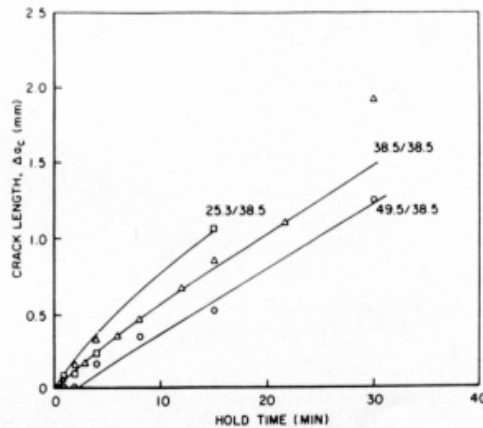


Figure A11- IN100 Crack length versus hold time plots for different K_{\max} values for fatigue and constant initial K_{applied} for the hold time [Larsen and Nicholas, 1983].

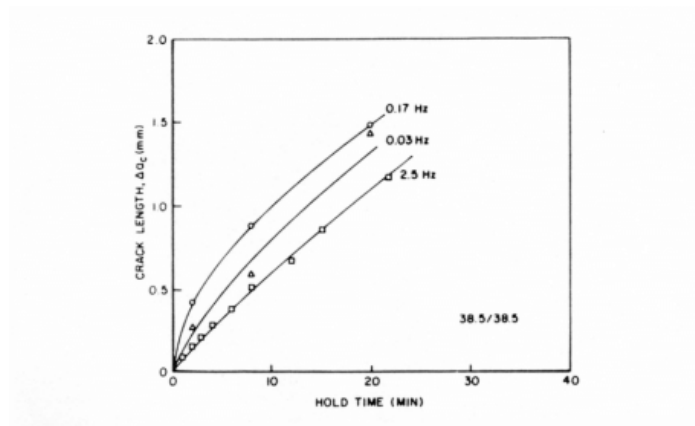


Figure A12- IN100 Crack length versus hold time for different frequencies of fatigue cycling at a constant value of K_{max} applied during fatigue and K applied initially during the hold time [Larsen and Nicholas, 1983].

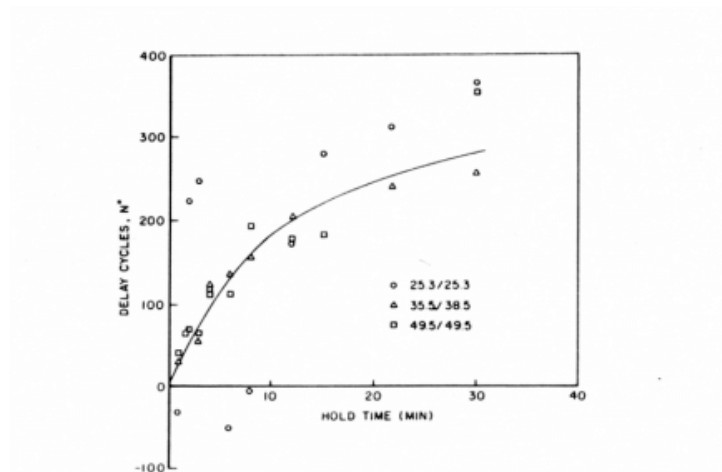


Figure A13.-IN100 Fatigue crack growth delay cycles versus hold time for various K_{max} applied during fatigue and K applied initially during the hold time. The data exhibit a high degree of scatter [Larsen and Nicholas, 1983].

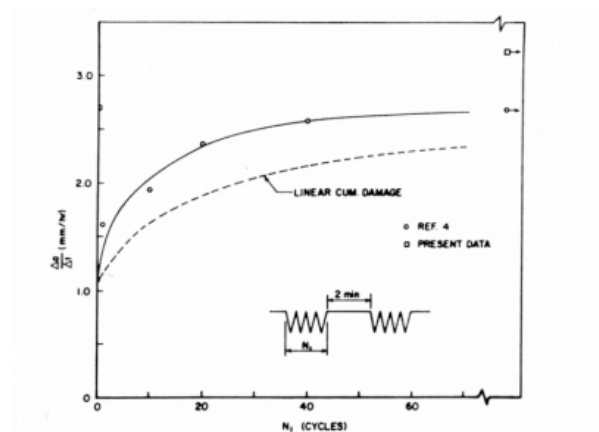


Figure A14- IN100 Crack growth versus the number of cycles applied between hold times of two minutes. The dashed line is an estimation of growth rate using the steady-state creep and fatigue crack growth rate with no interaction effects [Larsen and Nicholas, 1983].

References for IN100

- N.E. Ashbaugh, 1983, "Effect of Through-the-Thickness Stress Distribution upon Crack Growth Behavior in a Nickel-Base Superalloy," *Fracture Mechanics, Fourteenth Symposium – Volume II: Testing and Applications, ASTM STP 791*, Vol. II, pp. II-517-II-535.
- K.H.G. Ashbee, 1997, "Shear Creep of Aircraft Gas Turbine Alloys," *Journal of Materials Science Letters (UK)*, Vol. 16, pp. 1444-1445.
- A. Baldan, 1992, "Effects of Grain Size and Carbides on the Creep Resistance and Rupture Properties of a Conventionally Cast Nickel-Base Superalloy," *Zeitschrift fur Metallkunde (Germany)*, Vol. 83, pp. 750-757.
- K.S. Chan, J. Lankford, 1988, "The Role of Microstructural Dissimilitude in Fatigue and Fracture of Small Cracks," *Acta Metallurgica*, Vol. 36, pp. 193-206.
- J.P. Dennison, P.D. Holmes, B. Wilshire, 1978, "The Creep and Fracture Behavior of the Cast, Nickel-based Superalloy, IN100," *Materials Science and Engineering*, Vol. 33, pp. 35-47.
- R.C. Donath, T. Nicholas, and L.U. Fu, 1981, "An Experimental Investigation of Creep Crack Growth in IN100," *Fracture Mechanics: Thirteenth Conference, ASTM STP 743*, pp. 186-206.
- T. Hinnerichs, A. Palazotto, T. Nicholas, 1981, "Application of a Numerical Procedure to Creep Crack Growth From Displacement Measurements in IN100," *Fracture Mechanics, 14th Symposium, Vol. 2, Testing and Applications, Los Angeles, Calif., U.S.A*, Vol. 2, pp. 166-181.
- D. Krajcinovic, S. Selvaraj, 1984, "Creep Rupture of Metals--an Analytical Model," *Journal of Engineering Materials and Technology*, Vol. 106, pp. 405-409.
- J.M. Larsen, T. Nicholas, 1983, "Load Sequence Crack Growth Transients in a Superalloy at Elevated Temperature," *Fracture Mechanics, Fourteenth Symposium – Volume II: Testing and Applications, ASTM STP 791*, vol. II, pp. II-536-II-552.
- C.M. Potter, J.A. Spittle, 1979, "The Effect of Casting Conditions on the Morphology of the gamma ' Precipitate in the Nimonic Alloy IN100," *Phase Transformations*, Vol. 2.
- G.R. Romanoski Jr., R.M. Pelloux, 1990, "The Fatigue Behavior of Small Cracks in an Aircraft Turbine Disk Alloy," *Elevated temperature crack growth; Proceedings of the Symposium, ASME Winter Annual Meeting, Dallas, TX*, pp. 7-23.
- S. Rupp, Y. Bienvenu, L. Ouichou, G. Lesoult, 1986, "A Solidification Study of IN100 Type Superalloys with Varying Ti and C Contents," *High temperature alloys for gas turbines and other applications 1986; Proceedings of the Conference, Liege, Belgium*, pp. 757-766.
- B. J. Schwartz, C.G. Annis, Jr., 1983, "A Synergistic Fracture Mechanics Approach to Fatigue Life Evaluation," *Engineering Fracture Mechanics*, Vol. 18, pp. 815-826.

M. Tabuchi, K. Kubo, K. Yagi, 1993, "Creep Crack Growth of Creep Brittle Alloy," *Creep and Fracture of Engineering Materials and Structures*, Swansea, UK, 28 Mar.-2 Apr. 1993, pp. 449-458.

J.N. Yang, R.C. Donath, 1984, "Statistics of Crack Growth of a Superalloy Under Sustained Load," *ASME, Transactions, Journal of Engineering Materials and Technology*, Vol. 106, pp. 79-83.

Rene 95

Much of the research focus on Rene 95 has been on the environment and microstructure effects on crack growth rates at high temperatures. Both have a large influence on the crack growth rates and there is interaction between them since certain microstructures are more susceptible to environmental effects than others.

Figure A15 shows the large differences in creep crack growth rates for several nickel base superalloys tested in air at 649°C. In an inert environment, the CCGRs are almost the same; however, in air, grain boundary oxidation is present to a different extent on the varying microstructures of the nickel base superalloys and depends on the structure and composition of the grain boundaries. The reduction of CCGR in an inert atmosphere at 650°C compared to air can be up to a 1000 times [Bain and Pelloux, 1984] (Figure A16). Even a specimen tested in Argon at a relatively high stress level has a lower CCGR than a specimen tested at the same or lower stress level in air (Figure A17). Because of the effects of oxidation, CCGR can be K independent for low values of da/dt , Fig. A18, [Bain and Pelloux, 1984]. The two stage behavior of da/dt versus K in the air atmosphere is not present in the inert atmosphere. Even though there is a large amount of scatter in plots such as figure A16, the overall creep crack growth rate may be a unique function of K for Rene 95.

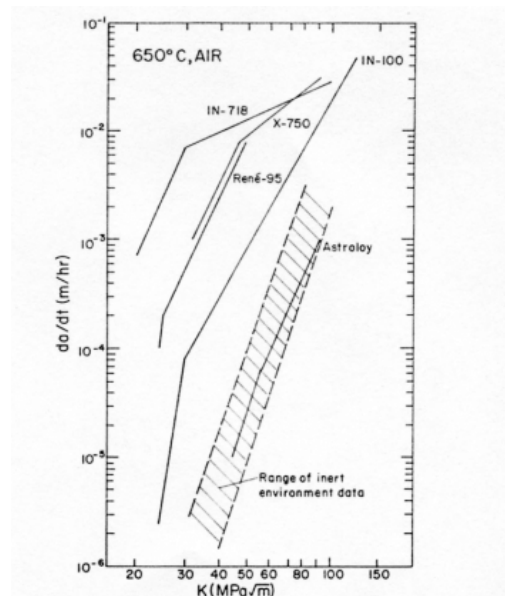


Figure A15- A large difference of CCGR versus K_I behavior of several nickel-base superalloys tested in air at 650°C [Bain and Pelloux, 1984].

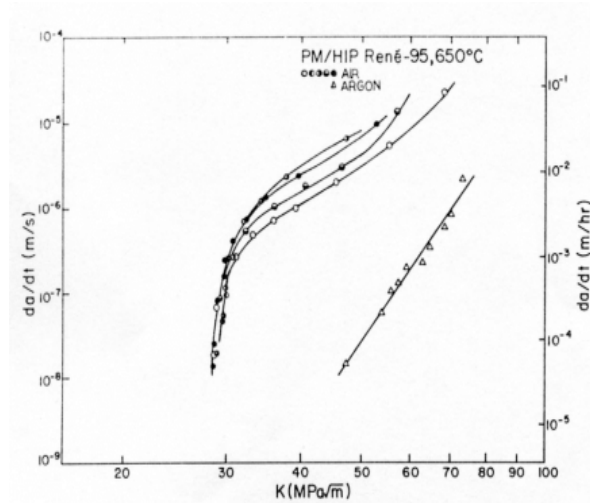


Figure A16- Creep crack growth rate data for PM/HIP Rene 95 tested at 650°C in air and purified argon, indicating a reduction in CCGR in the argon atmosphere [Bain and Pelloux, 1984].

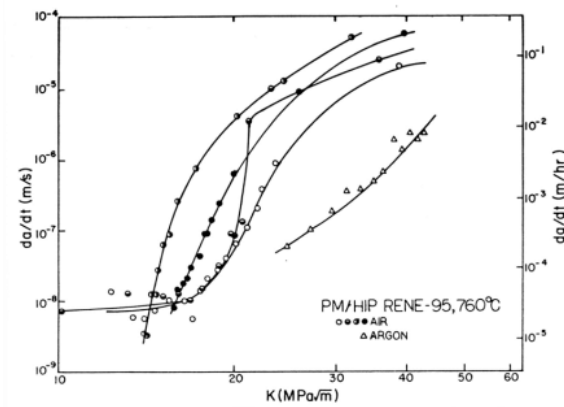


Figure A17- Creep crack growth rate data for PM/HIP Rene 95 tested at 760°C in air and purified argon, indicating a reduction in CCGR in the argon atmosphere and also showing a large scatter in the CCGR in air data [Bain and Pelloux, 1984].

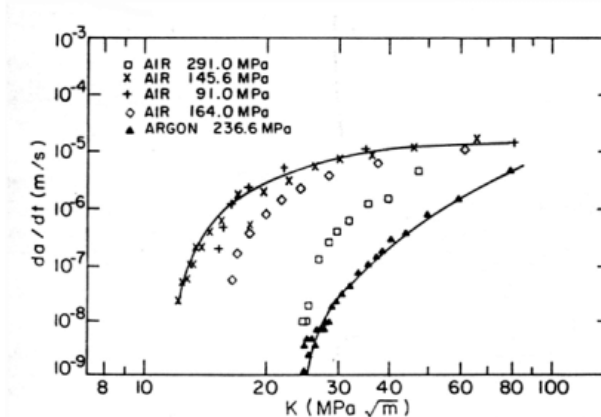


Figure A18- Crack growth rates for Rene 95 tested in air at different stress levels compared to Rene 95 tested in an argon atmosphere [Bain and Pelloux, 1984].

Figure A19 shows how the crack growth rates in Region II increase with increasing R-ratio at 538°C in Rene 95. Crack growth is dependent on the loading waveform and on K dependent crack closure effects; closure may be from oxide layers building up or plasticity in the vicinity of the crack tip [Van Stone and Krueger, 1986]. Crack growth rate also accelerates with increased hold time (Figure A20), and it can be modeled using superposition of the cyclic crack growth and the time dependent crack growth [Van Stone, 1990]. Figure A20b is plotted on linear axes because of the linear nature of the superposition rule; also, $R=0$ so K_{max} is the same as ΔK . The type of test can be a factor in the da/dN versus ΔK behavior (Figure A21); tests run at load control and ΔK control show similar results while the data for constant ΔK experiments lie well below the load control and ΔK data. There is probably a significant amount of retardation that occurred at the crack tip for the rapid crack growth rates [Van Stone, 1990].

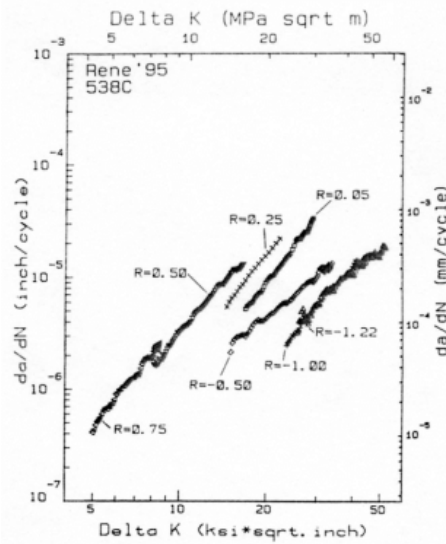


Figure A19- Rene 95 crack growth data at 538°C, showing crack growth rates that increase with increasing R-ratio, [VanStone and Kruger, 1986]

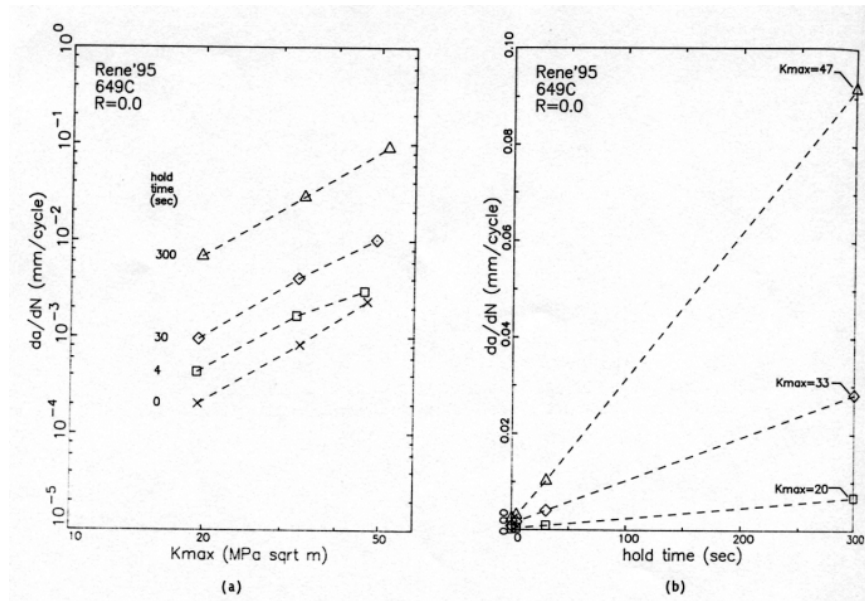


Figure A20-a) Crack growth rate versus K_{max} of Rene 95 tested at 649°C with $R=0$, which shows increasing crack growth rate with increasing hold time; b) crack growth rate versus hold time for different hold times, fitting the data trend with a superposition model.

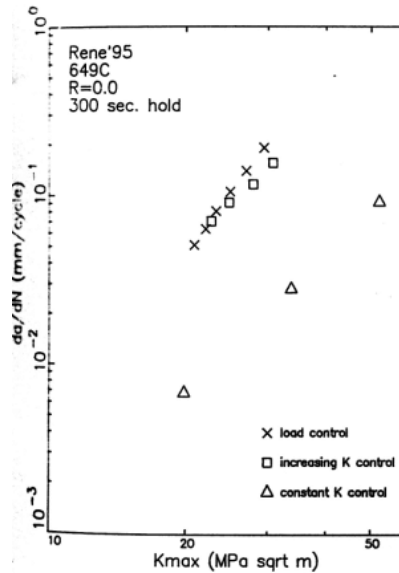


Figure A21- The effect of test control mode on crack growth rates in Region II for Rene 95 specimens tested at 649°C with a 300 second hold time, showing significant retardation in the constant ΔK control mode.

Microstructure features such as grain size and γ' size and shape among others can have a significant influence on the failure mode and the crack growth rates of Rene 95. Figures A22 and A23 indicate that the cyclic crack growth for extrusion and forged and HIP microstructures is larger than for a wrought and cast microstructure. In the fine grain microstructures of the extrusion and forged and HIP conditions, the failure mode is

intergranular while the large grains for the wrought and cast microstructure lead to intragranular failure. This may be because environmentally assisted cracking has more of an affect in fine grain microstructures [Miner and Gayda, 1984]. Additionally, a “crossover” behavior may be seen in Rene 95 for specimens with large grain sizes and large γ' sizes (Figure A24). However, this affect is seen in a variety of microstructure conditions; therefore, crossover may be related to local crack tip blunting through creep and cyclic plasticity and is not necessarily microstructure dependent [Van Stone and Krueger, 1986].

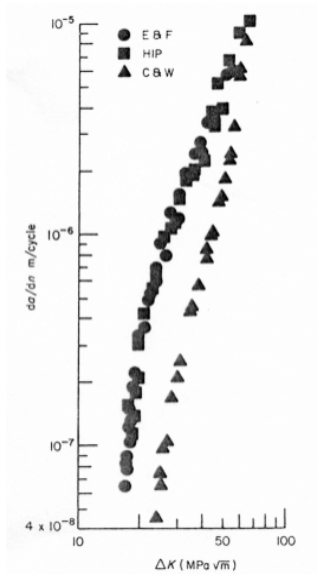


Figure A22- Cyclic crack growth of Rene 95 at 540°C for extruded-and-forged, hot-isostatically-pressed, and cast-and-wrought samples, showing slightly dissimilar behavior for the cast-and-wrought data.

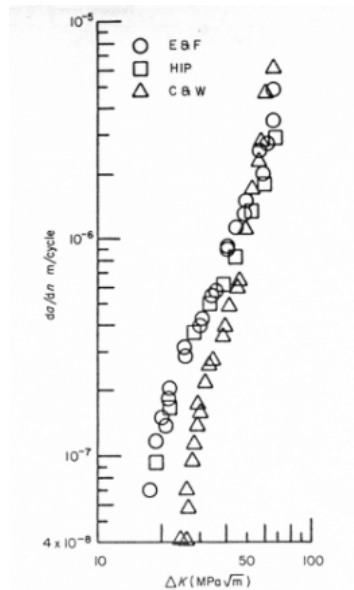


Figure A23- Cyclic crack growth of Rene 95 at 650°C for extruded-and-forged, hot-isostatically-pressed, and cast-and-wrought samples, showing slightly dissimilar behavior for the cast-and-wrought data.

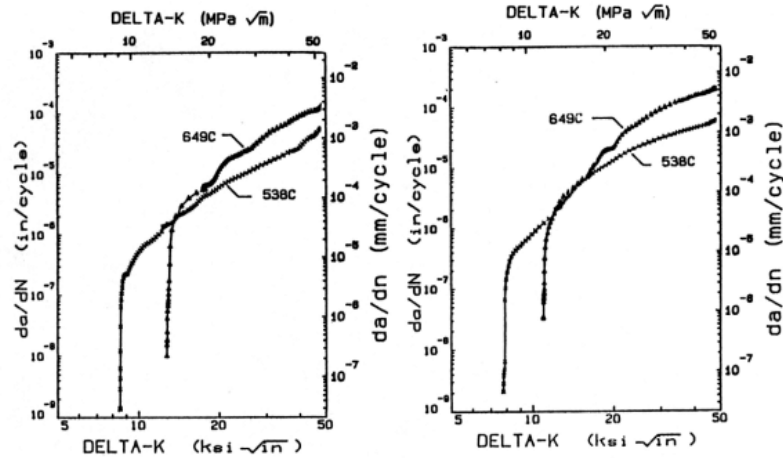


Figure A24- Crossover behavior for fatigue crack growth of HIP-compacted Rene 95 with a) enlarged grain size and b) enlarged γ' precipitate size.

Rene 95 References

- G. Arslan, M. Doruk, 1998, "Cyclic Crack Growth Behaviour of Two Nickel Base Turbine Disc Alloys," *Journal of Materials Science*, Vol. 33, pp. 2653-2658.
- N.E. Ashbaugh, "Effects of Load History and Specimen Geometry on Fatigue Crack Closure Measurements," 1988, *Mechanics of fatigue crack closure*. Philadelphia, PA, American Society for Testing and Materials, pp. 186-196.
- K.R. Bain, R.M. Pelloux, 1984, "Effect of Environment on Creep Crack Growth in PM/HIP Rene-95," *Metallurgical Transactions A*, Vol. 15A, pp. 381-388.
- J. Bartos, S.D. Antolovich, 1977, "Effect of grain size and gamma-prime size on fatigue crack propagation in Rene 95," *Advances in research on the strength and fracture of materials; Proceedings of the Fourth International Conference on Fracture, Waterloo, Ontario, Canada*, Vol. 2B, pp. 995-1005.
- K.J. Hsia, A.S. Argon, D.M. Parks, 1992, "Dominant Creep Failure Process in Tensile Components," *Journal of Engineering Materials and Technology*, Vol. 114, pp. 255-264.
- J.F. McCarver, R.O. Ritchie, 1982, "Fatigue Crack Propagation Thresholds for Long and Short Cracks in Rene 95 Nickel-Base Superalloy," *Materials Science and Engineering*, Vol. 55, pp. 63-67.
- R.V. Miner, J. Gayda, 1984, "Effects of Processing and Microstructure on the Fatigue Behavior of the Nickel-base Superalloy Rene 95," *Int. J. Fatigue*, Vol. 6, pp. 189-193.
- R.H. Van Stone, D.D. Krueger, 1986, "Near-Threshold Crack Growth in Nickel-Base Superalloys," *Fracture Mechanics: Nineteenth Symposium, San Antonio, Texas, USA*, pp. 883-906.
- R.H. Van Stone, 1990, *Elevated temperature crack growth; Proceedings of the Symposium, ASME Winter Annual Meeting, Dallas, TX*, pp. 53-68.

L.P. Zawada, T. Nicholas, 1988, "The Effect of Loading History on Closure Behavior in Rene 95," *Fracture mechanics. Philadelphia, PA, American Society for Testing and Materials*, pp. 192-205.

L.P. Zawada, T. Nicholas, 1988, "The Effect of Closure on the Near-Threshold Fatigue Crack Propagation Rates of a Nickel Base Superalloy," *Mechanics of fatigue crack closure. Philadelphia, PA, American Society for Testing and Materials*, pp. 548-567.

Rene 88

The small amount of data available on Rene 88 relates microstructure and heat treatments to creep and fatigue crack growth properties. Kissinger, 1996, used two-step cooling paths from the solutionizing temperature to attain different γ' size distributions. The transition temperature of the heat treatment also influences the mechanical properties. Figure A25 shows the minimum creep rate plotted against transition temperature. The four data points also represent different microstructures. The crack growth rate data also shows a dependence on the transition temperature (Figure A26); since the specimens cooled at 1900°F show a higher minimum creep rate, there is significant stress relaxation at the crack tip under creep fatigue conditions [Kissinger, 1996]. The hold time fracture surfaces showed the fracture path was primarily intergranular, which may imply the environment also has some interaction with the crack growth behavior.

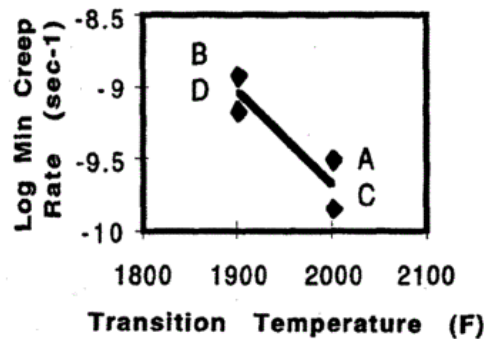


Figure A25- Rene 88dt data showing the influence on the minimum creep rate of different γ' size distributions and transition temperatures in a two step cooling heat treatment.

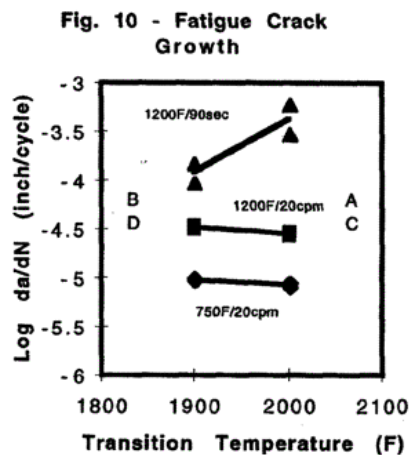


Figure A26- Effect of temperature and microstructure on the crack growth rates for different waveforms and hold times.

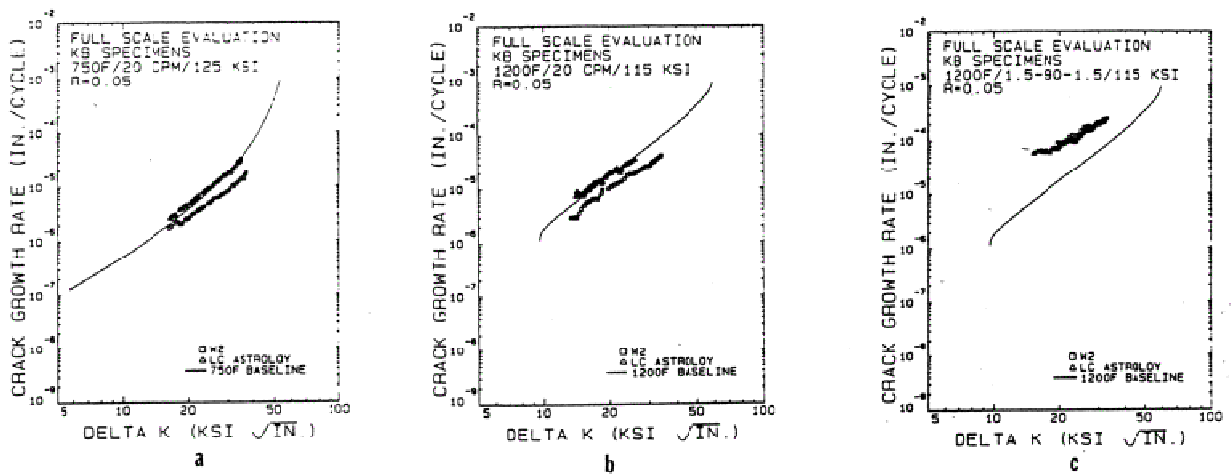


Figure A27- Fatigue crack growth rates for Rene 88dt and Astroloy forgings for a) 750°F/20cpm, b) 1200°F/20cpm, and c) 1200°F/1.5-90-1.5. The data is compared to Rene 95 with the same waveforms.

References for Rene 88

- R.D. Kissinger, 1996, "Cooling Path Dependent Behavior of a Supersolvus Heat Treated Nickel Base Superalloy," *Superalloys 1996; Proceedings of the 8th International Symposium, Champion, PA, Sept. 22-26, 1996*, pp. 687-695.
- D.D. Krueger, R.D. Kissinger, and R.G. Menzies, 1992, "Development and Introduction of a Damage Tolerant High Temperature Nickel-base Disk Alloy, Rene 88DT," *Superalloys 1992; Proceedings of the 7th International Symposium, Champion, PA, Sept. 20-24, 1992*, pp. 277-286.
- S.T. Wlodek, M. Kelly, D.A. Alden, 1996, "The Structure of Rene 88 DT," *Superalloys 1996; Proceedings of the 8th International Symposium, Champion, PA*, pp. 129-136.

Waspaloy

Much of the Waspaloy research has been on the frequency and temperature effects on creep fatigue crack growth. When da/dN is plotted against ΔK , there is a large variation in the data at different temperatures and frequencies. Figure A28 shows the temperature dependence of da/dN versus ΔK . Though da/dN versus ΔK data may be different for different temperatures and frequencies, the data may follow parallel trends (Figure A29), which may indicate that either fatigue cycling or creep crack growth is the dominant crack growth mechanism in the range of frequencies and temperatures tested. However, Branco, 1996, showed a larger variation of da/dN versus K_{max} with frequency (Figure A30); crack growth under a high temperature cyclic stress may be divided into three regimes: cycle dependent or frequency independent at high frequencies, frequency dependent where both time dependent and cyclic crack growth become important, and time dependent or frequency independent at low frequencies. Furthermore, increasing ΔK increases the frequency where the crack growth goes from being frequency dependent to cycle dependent [Branco, 1996]. Failure at high frequencies is predominantly transgranular while the primary failure mechanism for the more time dependent low frequencies is intergranular [Branco, 1996], possibly because there is more time for oxidation at the grain boundaries. Figure A31 shows influence of stress ratio on crack propagation as seen in experiment and modeled using a hyperbolic sine function.

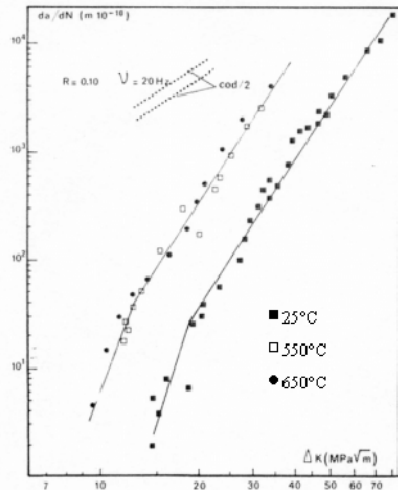


Figure A28- FCGR for Waspaloy versus ΔK at different temperatures, which shows that Waspaloy exhibits a high temperature dependence.

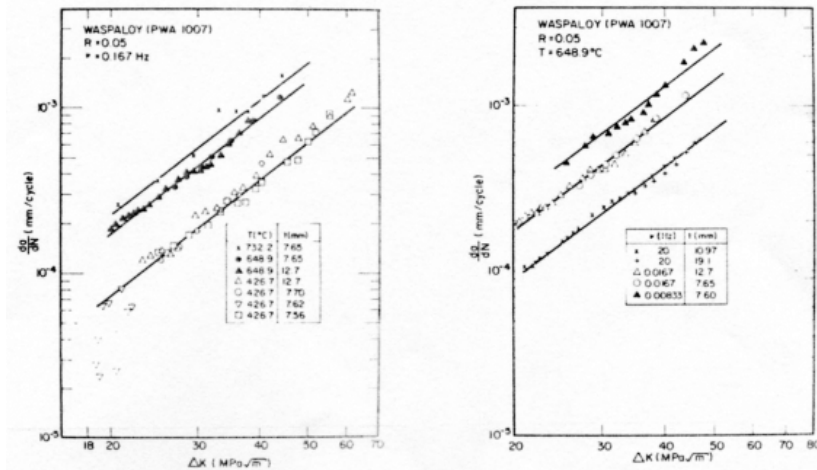


Figure A29- a) Effect of temperature on fatigue crack growth rate in Waspalloy, $\nu=0.167$ Hz; b) Effect of frequency on FCGR in Waspalloy, $T=649^{\circ}\text{C}$.

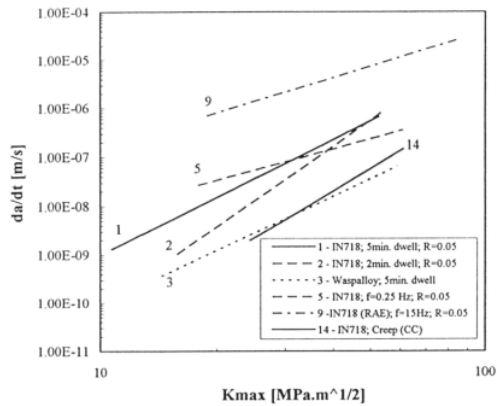


Figure A30- da/dt versus K_{max} for Waspalloy and IN718 specimens tested at $R=0.05$ and different frequencies. There is a large variation in da/dt data with frequency.

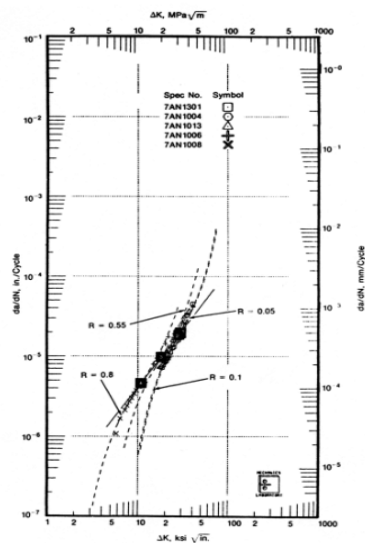


Figure A31- Waspalloy crack propagation versus ΔK at 1200°F and 0.1667 Hz at different R values modeled using different stress ratios

Waspalloy References

- C. Moura Branco, 1996, “Elevated Temperature: Fatigue Crack Growth of Nickel Base Superalloys: A Review and Modelling,” *Mechanical Behavior of Materials at High Temperature; Proceedings of the NATO Advanced Study Institute, Sesimbra, Portugal*, pp. 93-134.
- M. Clavel, A. Pineau, 1981, “Fatigue Behavior of Two Nickel-base Alloys I: Experimental Results on Low Cycle Fatigue, Fatigue Crack Propagation and Substructures,” *Materials Science and Engineering*, Vol. 55, pp. 157-171.
- Kitagawa, Masaki, 1989, “Life Prediction and Fatigue,” *Superalloys, Supercomposites and Superceramics*, pp. 413-437.
- Y. Lindblom, G. Enberg, 1982, “Creep Damage and Fracture (in Wrought and Cast Precipitation-hardened Superalloys),” *High temperature alloys for gas turbines 1982; Proceedings of the Conference, Liege, Belgium*, pp. 447-467.
- H.W. Liu, J.J. McGowan, 1981, “A Kinetic Analysis of High Temperature Fatigue Crack Growth,” *Scripta Metallurgica*, Vol.15, pp. 507-512.
- B.J. Schwartz, C.B. Annis, Jr., 1983, “A Synergistic Fracture Mechanics Approach to Fatigue Life Evaluation,” *Engineering Fracture Mechanics*, Vol. 18, pp. 815-826.